our model cannot distinguish the differences in chemical structure of substrates. In addition, a valence of net charge of substrate is not considered in this model because of no information. Therefore, there may be substrates for which transport features do not fit the simulation by our model. Further studies concerning structure–activity relationship are necessary to increase the comprehensiveness of the model.

Effects of the membrane potential

As described in Methods, 8 of 10 rate constants and the concentrations of charged molecules were defined as voltage-dependent. Based on this, the voltage dependence of Gly-Sar transport can be interpreted as follows. Concerning current–voltage (I–V) profiles (Fig. 4*B*), when the concentration of Gly-Sar was increased, the principal step limiting the rate of the transport cycle shifts from the transition of PEPT1 carrying both H^+ and Gly-Sar (k_7 and k_8 in Fig. 3*A*) to that of empty PEPT1 (k_1 and k_2), i.e. from the voltage-independent step to the dependent one. Therefore, the currents induced by a higher concentration of Gly-Sar exhibited more intensive voltage dependence. On the other hand, the voltage dependence of K_m value for Gly-Sar seems to be due to two causes: (1) H^+ exhibits the inductive and inhibitory effects, (2) H^+ concentrations

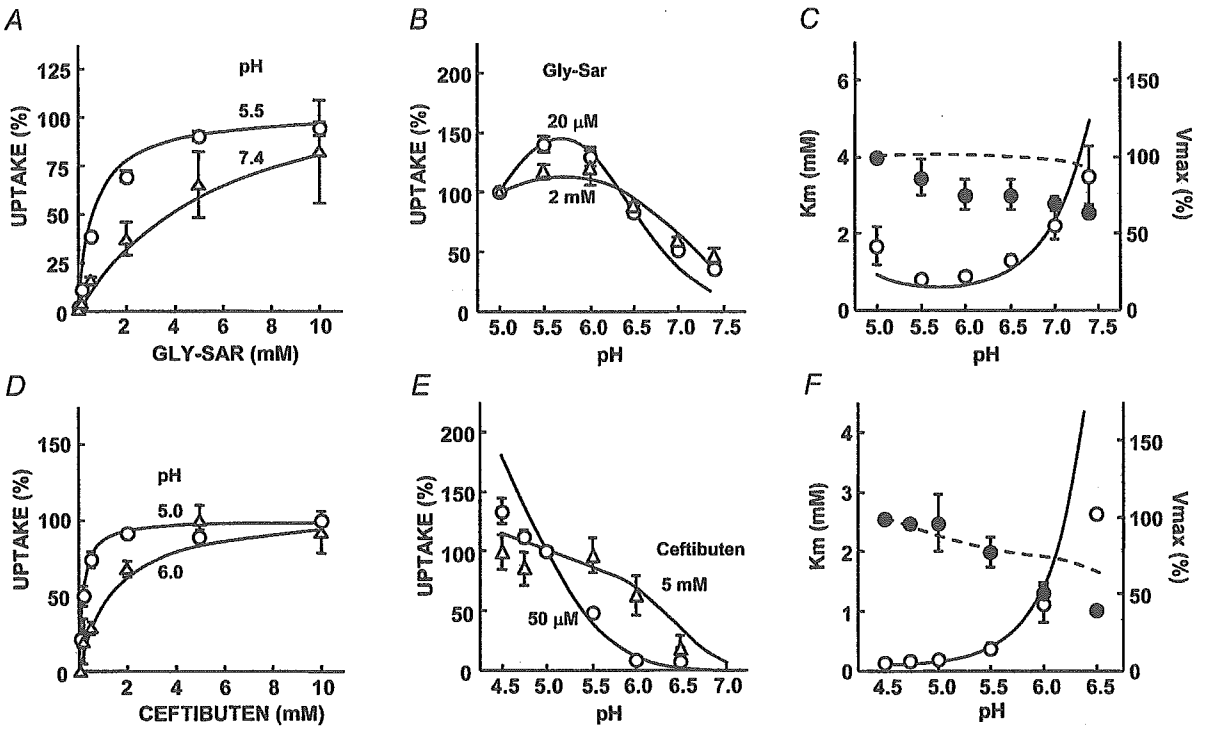

Figure 5. Simulation of Gly-Sar and ceftibuten uptake in Caco-2 cells
A–F, the curves were obtained by simulation at 37°C and −57 mV, and the symbols represent the experimental data. *A*, concentration dependence of Gly-Sar uptake by PEPT1. The transport of Gly-Sar at pH 5.5 and 7.4 was calculated by simulation (curves) at concentrations from 2 μM to 10 mM (every 2 μM). [^{3}H]Gly-Sar uptake at pH 5.5 (○) or pH 7.4 (△) was measured in Caco-2 cells at 37°C, and normalized to the respective V_{max} values. *B*, pH dependence of Gly-Sar transport by PEPT1. pH profiles of Gly-Sar transport were delineated by simulation (curves) at 20 μM and 2 mM Gly-Sar. In simulation, the transport of Gly-Sar was calculated every 0.01 pH unit. 20 μM (○) and 2 mM (△) [^{3}H]Gly-Sar uptake was measured in Caco-2 cells at various pH values. *C*, pH dependence of K_m and V_{max} values for Gly-Sar transport. In simulation, V_{max} (dashed line) was assumed as the transport of 50 mM Gly-Sar, and was normalized to the value at pH 5.0, and K_m values (continuous line) were estimated by calculation of substrate concentration which displayed the transport of 50% V_{max}. K_m (○) and V_{max} (●) values obtained experimentally. *D*, concentration dependence of ceftibuten transport via PEPT1. The transport of ceftibuten at pH 5.0 and 6.0 was simulated (curves) similar to *A*. Ceftibuten uptake was measured at pH 5.0 (○) and 6.0 (△) in Caco-2 cells, and normalized to the respective V_{max} values. *E*, pH profiles of 50 μM and 5 mM ceftibuten transport by PEPT1. The simulation of pH dependence of ceftibuten transport was performed similar to *B* (curves). 50 μM (○) and 5 mM (△) ceftibuten uptake was measured in Caco-2 cells at various pH values. *F*, pH dependence of K_m and V_{max} values for ceftibuten transport by PEPT1. V_{max} (dashed line) was assumed as the uptake of 50 mM ceftibuten, and was normalized to the value at pH 4.5. K_m values (continuous line) were determined similar to *C*. Four dissociation constants of ceftibuten on the exterior side ($K_{d,Soc1}$, $K_{d,Soc2}$, $K_{d,Son}$ and $K_{d,Soa}$ in Fig. 3*A*) are all 50 μM.

at both H^+- and substrate-binding sites are increased by the negative membrane potential. Thus, the profile of the voltage dependence of K_m value is variable in terms of pH, i.e. at pH 7.0, the inductive effect was well elicited by hyperpolarization, resulting in a decrease of K_m, whereas the inhibitory effect was predominant at pH 5.0 and the K_m value increased.

Compared with other symporters, PEPT1 is ordered to accept diverse physiological substrates, more than 8000 types of di/tripeptides with a variety of charges, and anionic compounds in particular are generally disadvantageous to enter cells because of negative membrane potential. Therefore, protonation of the substrate-binding site may be a distinctive feature for PEPT1 to overcome the difficulty in the transport of anionic substrates. Considering the slightly acidic pH of the small intestine (Adibi, 1997), the protonation of the substrate-binding site seems to be a dexterous strategy to enable the transport of differently charged substrates with high activity.

Stoichiometry

Previous studies demonstrated that not only neutral and cationic substrates, but also anionic substrates, induced inward currents via PEPT1 (Mackenzie *et al.* 1996*a*; Amasheh *et al.* 1997). The following hypotheses about the stoichiometry of anionic substrates have been suggested: (1) before transport, an anionic substrate undergoes protonation, thus the stoichiometry of anionic substrate

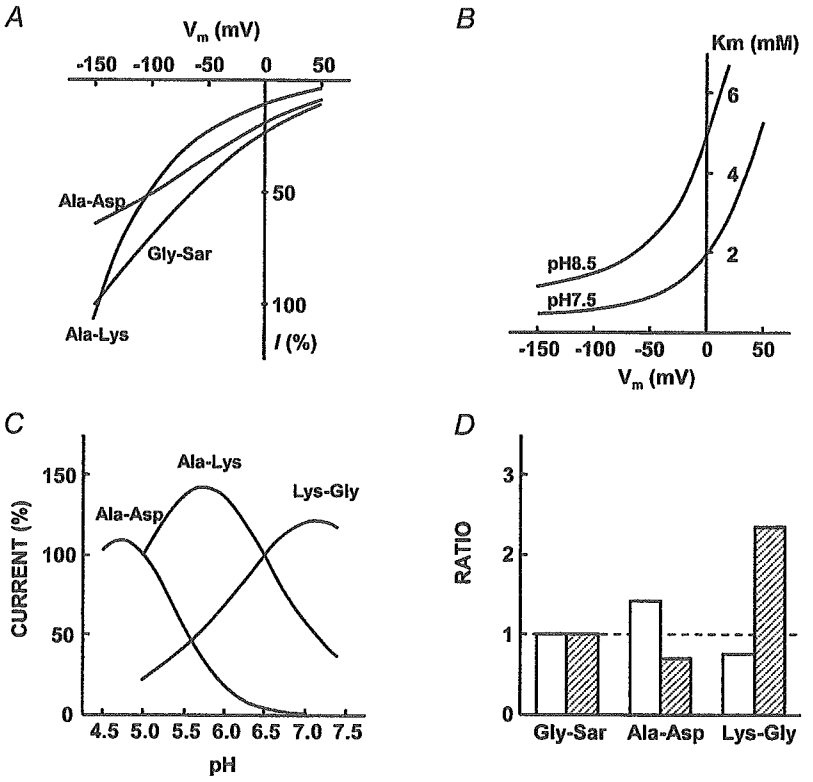

Figure 6. Simulation of the transport properties for various charged substrates
A, current–voltage profiles for neutral and charged substrates. The current–voltage relationship was delineated by simulation for 10 mM Gly-Sar, Ala-Asp and Ala-Lys at pH 6.0, with normalization of each value to that of Gly-Sar at −150 mV. The pK_a values of Ala-Asp (pK_{a1} = 3.0, pK_{a2} = 4.4, pK_{a3} = 8.1) and Ala-Lys (pK_{a1} = 3.2, pK_{a2} = 7.7, pK_{a3} = 10.5) were obtained from a previous study (Mackenzie *et al.* 1996*a*). Four dissociation constants ($K_{d,Soc1}$, $K_{d,Soc2}$, $K_{d,Son}$ and $K_{d,Soa}$ in Fig. 3*A*) of Ala-Asp were 200 μM, and those of Ala-Lys were defined as 1 mM, except for $K_{d,Soc1}$ = 100 mM. *B*, voltage dependence of K_m values for Lys-Gly. Voltage dependence of K_m for Lys-Gly was simulated similar to Fig. 3*C* using pK_a values of Lys-Gly (pK_{a1} = 3.0, pK_{a2} = 8.1, pK_{a3} = 10.7) (Kottra *et al.* 2002) and four dissociation constants defined as 3 mM. *C*, pH dependence of currents evoked by charged substrates via PEPT1. pH profiles of currents induced by Ala-Asp, Ala-Lys and Lys-Gly were simulated similar to Fig. 5*B* at 20 μM, −60 mV. The magnitude of currents was normalized to that at pH 5.0 for Ala-Asp and Ala-Lys, and at pH 6.5 for Lys-Gly. *D*, the transport ratio of H^+ to substrate (open bar) and the ratio of the total currents induced by substrate flux to the charge movement by H^+ flux (hatched bar) were calculated using the simulator at 1 mM substrate concentration, −60 mV and pH 5.0.

to H^+ is 1 : 2 (Steel *et al.* 1997; Kottra *et al.* 2002); (2) the transport of an anionic substrate with one H^+ is accompanied by a counterflux of a negatively charged ion, which elicits an inward current (Mackenzie *et al.* 1996*a*); and (3) PEPT1 transports only substrate in neutral form (Wenzel *et al.* 1996). However, our studies demonstrated that ceftibuten exists as monoanion or dianion, suggesting that PEPT1 can transport substrates with a negative charge. Although our experimental data can not exclude the possibility of protonation of substrate before permeation via PEPT1 and that of a counterflux of a negatively charged ion, it seems unlikely that protonation of substrate or a counterflux of an anion occurs only in the case of the transport of negatively charged substrate. In the present study, we suggested that the stoichiometry of anionic substrate to H^+ is 1 : 2 because of the simultaneous transport of H^+ at both H^+- and substrate-binding sites. By this model, the inward currents with the transport of Ala-Asp can be obtained (Fig. 6*A*). In addition, the coupling ratio of a neutral substrate to H^+ was defined as 1, and that of a cationic substrate as 1 (k_5 and k_6 in Fig. 3*A*) or 0 (k_3 and k_4). The different stoichiometry in terms of the charges of substrates is apparent in Fig. 6*D*. The ratio of H^+ to anionic substrate was above 1, but that to cationic one was under 1, and the odd values are as a consequence of the proportion of ionic species. Similarly, the large current of Lys-Gly and the small one of Ala-Asp can be interpreted by the cotransport of H^+ and Lys-Gly carrying a positive charge, and the offset of charge movement of H^+ by the net negative charge of Ala-Asp, respectively. These results are consistent with previous studies demonstrating that currents evoked by cationic substrates were greater and that the intracellular acidification by basic and acidic dipeptides was more moderate and rapid than that by neutral ones, respectively (Steel *et al.* 1997; Kottra *et al.* 2002).

Our proposed mechanisms, such as the binding of H^+ to the substrate-binding site, are not completely proved by experiments, but previous studies demonstrated that the histidine residue in the transmembrane domain of PEPT1 is involved in the substrate-binding site (Terada *et al.* 1996, 1998; Chen *et al.* 2000), which may support the protonation of substrate-binding site. Crystallization of PEPT1 protein may be the promising strategy to evaluate our suggested transport mechanisms of PEPT1.

In conclusion, based on experiments and information from the literature, we proposed the binding of H^+ to the substrate-binding site and constructed a transport model of PEPT1 for neutral and charged substrates. Computational simulation reproduced well the concentration-, pH- and voltage-dependent transport of Gly-Sar and pre-steady-state currents by PEPT1. Moreover, various transport properties of negatively and positively charged substrates could be obtained. These findings indicate the possibility of the proposed transport mechanisms of PEPT1, and suggest that computational modelling is a useful strategy to validate the mechanisms presumed.

References

Adibi SA (1997). The oligopeptide transporter (Pept-1) in human intestine: biology and function. *Gastroenterology* **113**, 332–340.

Amasheh S, Wenzel U, Boll M, Dorn D, Weber W-M, Clauss W & Daniel H (1997). Transport of charged dipeptides by the intestinal H^+/peptide symporter PepT1 expressed in *Xenopus laevis* oocytes. *J Membr Biol* **155**, 247–256.

Chen X-Z, Steel A & Hediger MA (2000). Functional roles of histidine and tyrosine residues in the H^+-peptide transporter PepT1. *Biochem Biophys Res Commun* **272**, 726–730.

Daniel H (2004). Molecular and integrative physiology of intestinal peptide transport. *Annu Rev Physiol* **66**, 361–384.

Daniel H & Kottra G (2004). The proton oligopeptide cotransporter family SLC15 in physiology and pharmacology. *Pflugers Arch* **447**, 610–618.

Eskandari S, Loo DDF, Dai G, Levy O, Wright EM & Carrasco N (1997). Thyroid Na^+/I^- symporter. Mechanism, stoichiometry, and specificity. *J Biol Chem* **272**, 27230–27238.

Fei Y-J, Kanai Y, Nussberger S, Ganapathy V, Leibach FH, Romero MF, Singh SK, Boron WF & Hediger MA (1994). Expression cloning of a mammalian proton-coupled oligopeptide transporter. *Nature* **368**, 563–566.

Forster I, Hernando N, Biber J & Murer H (1998). The voltage dependence of a cloned mammalian renal type II Na^+/P_i cotransporter (NaP_i-2). *J General Physiol* **112**, 1–18.

Grasset E, Pinto M, Dussaulx E, Zweibaum A & Desjeux J-F (1984). Epithelial properties of human colonic carcinoma cell line Caco-2: electrical parameters. *Am J Physiol Cell Physiol* **247**, C260–C267.

Guo A, Hu P, Balimane PV, Leibach FH & Sinko PJ (1999). Interactions of a nonpeptidic drug, valacyclovir, with the human intestinal peptide transporter (hPEPT1) expressed in a mammalian cell line. *J Pharmacol Exp Ther* **289**, 448–454.

Inui K & Terada T (1999). Dipeptide transporters. In *Membrane Transporters as Drug Targets*, ed. Amidon GL & Sadée W, pp. 269–288. Kluwer Academic/Plenum Publishers, New York.

Irie M, Terada T, Sawada K, Saito H & Inui K (2001). Recognition and transport characteristics of nonpeptidic compounds by basolateral peptide transporter in Caco-2 cells. *J Pharmacol Exp Ther* **298**, 711–717.

Kottra G, Stamfort A & Daniel H (2002). PEPT1 as a paradigm for membrane carriers that mediate electrogenic bidirectional transport of anionic, cationic, and neutral substrates. *J Biol Chem* **277**, 32683–32691.

Leibach FH & Ganapathy V (1996). Peptide transporters in the intestine and the kidney. *Annu Rev Nutr* **16**, 99–119.

Mackenzie B, Fei Y-J, Ganapathy V & Leibach FH (1996*a*). The human intestinal H^+/oligopeptide cotransporter hPEPT1 transports differently-charged dipeptides with identical electrogenic properties. *Biochim Biophys Acta* **1284**, 125–128.

Mackenzie B, Loo DDF, Fei Y-J, Liu W, Ganapathy V, Leibach FH & Wright EM (1996*b*). Mechanisms of the human intestinal H^+-coupled oligopeptide transporter hPEPT1. *J Biol Chem* **271**, 5430–5437.

Matsumoto S, Saito H & Inui K (1994). Transcellular transport of oral cephalosporins in human intestinal epithelial cells, Caco-2: interaction with dipeptide transport systems in apical and basolateral membranes. *J Pharmacol Exp Ther* **270**, 498–504.

Matsuoka S, Sarai N, Kuratomi S, Ono K & Noma A (2003). Role of individual ionic current systems in ventricular cells hypothesized by a model study. *Jpn J Physiol* **53**, 105–123.

Parent L, Supplisson S, Loo DDF & Wright EM (1992*a*). Electrogenic properties of the cloned Na^+/glucose cotransporter. I. Voltage-clamp studies. *J Membr Biol* **125**, 49–62.

Parent L, Supplisson S, Loo DDF & Wright EM (1992*b*). Electrogenic properties of the cloned Na^+/glucose cotransporter: II. A transport model under nonrapid equilibrium conditions. *J Membr Biol* **125**, 63–79.

Sawada K, Terada T, Saito H, Hashimoto Y & Inui KI (1999). Recognition of l-amino acid ester compounds by rat peptide transporters PEPT1 and PEPT2. *J Pharmacol Exp Ther* **291**, 705–709.

Steel A, Nussberger S, Romero MF, Boron WF, Boyd CAR & Hediger MA (1997). Stoichiometry and pH dependence of the rabbit proton-dependent oligopeptide transporter PepT1. *J Physiol* **498**, 563–569.

Terada T & Inui K (2004). Peptide transporters: structure, function, regulation and application for drug delivery. *Curr Drug Metab* **5**, 85–94.

Terada T, Saito H & Inui K (1998). Interaction of β-lactam antibiotics with histidine residue of rat H^+/peptide cotransporters, PEPT1 and PEPT2. *J Biol Chem* **273**, 5582–5585.

Terada T, Saito H, Mukai M & Inui K (1996). Identification of the histidine residues involved in substrate recognition by a rat H^+/peptide cotransporter, PEPT1. *FEBS Lett* **394**, 196–200.

Terada T, Sawada K, Saito H, Hashimoto Y & Inui K (1999). Functional characteristics of basolateral peptide transporter in the human intestinal cell line Caco-2. *Am J Physiol Gastrointest Liver Physiol* **276**, G1435–1441.

Wenzel U, Gebert I, Weintraut H, Weber W-M, Clauß W & Daniel H (1996). Transport characteristics of differently charged cephalosporin antibiotics in oocytes expressing the cloned intestinal peptide transporter PepT1 and in human intestinal Caco-2 cells. *J Pharmacol Exp Ther* **277**, 831–839.

Acknowledgements

This work was supported in part by the Leading Project for Biosimulation, and a Grant-in-Aid for Scientific Research from the Ministry of Education, Culture, Sports, Science and Technology of Japan. Megumi Irie is a Research Fellow of the Japan Society for the Promotion of Science.

Drug Metab. Pharmacokinet. 20 (3): 200–205 (2005).

Regular Article

Transcellular Transport of Creatinine in Renal Tubular Epithelial Cell Line LLC-PK$_1$

Yumiko URAKAMI, Naoko KIMURA, Masahiro OKUDA, Satohiro MASUDA, Toshiya KATSURA and Ken-ichi INUI

Department of Pharmacy, Kyoto University Hospital, Faculty of Medicine, Kyoto University, Kyoto, Japan

Full text of this paper is available at http://www.jstage.jst.go.jp/browse/dmpk

Summary: Background/Aim: Creatinine is excreted into urine via tubular secretion in addition to glomerular filtration. In the present study, characteristics of the creatinine transport in renal epithelial cells were investigated.

Methods: The transcellular transport and accumulation of [^{14}C]creatinine and [^{14}C]tetraethylammonium (TEA) were assessed using LLC-PK$_1$ cell monolayers cultured on porous membrane filters.

Results: [^{14}C]Creatinine was transported directionally from the basolateral to apical side of LLC-PK$_1$ cell monolayers. Basolateral uptake of [^{14}C]creatinine was dependent on membrane potential, and was saturable with apparent K_m and V_{max} values of 13.2 ± 2.8 mM and 13.1 ± 3.1 nmol/mg protein/5 min, respectively. Concomitant administration of organic cations (1 mM) such as cimetidine, quinidine and trimethoprim inhibited both the transcellular transport and accumulation of [^{14}C]creatinine. Furthermore, apical excretion of [^{14}C]creatinine was not dependent on acidification of the apical medium.

Conclusions: Creatinine was subjected to directional transport across renal epithelial cells from the basolateral to apical side. The organic cation transporter should be involved in the basolateral uptake of creatinine.

Key words: creatinine; LLC-PK$_1$; organic cation transporter; tetraethylammonium; transcellular transport; tubular secretion

Introduction

Creatinine (M.W.: 113.12, pKa: 4.8, 9.2) is a catabolic product of creatine, with both positive and negative charges, i.e. a zwitterion, at physiological pH. Because creatinine is excreted mostly into urine, its systemic clearance has been used for the evaluation of kidney function. Although the renal disposition of creatinine is mainly mediated by glomerular filtration, the secretion and reabsorption of creatinine at renal tubules have been also recognized.[1,2] The secretory fraction of creatinine is significant especially in patients with glomerular disorders,[3] and causes an overestimation of the glomerular filtration rate (GFR). Although organic ion transport systems have been implicated in the tubular secretion of creatinine, there is no evidence to reveal the transcellular transport of creatinine across the renal tubular epithelium.

In the proximal tubules of the kidney, organic ion transporters mediate elimination of cationic drugs into the urine.[4–7] According to studies using isolated membrane vesicles[8,9] and cultured renal epithelial cells,[10,11] the basolateral uptake of tetraethylammonium (TEA) is driven by the transmembrane potential difference. Subsequently, TEA is excreted across apical membranes by the H^+/organic cation antiporter. LLC-PK$_1$ cells, an established epithelial cell line derived from pig kidney, retain characteristics of the proximal tubular epithelium, and therefore they have been used for studying the tubular transport of various solutes including organic cations.[10–13] We demonstrated that the transcellular transport of TEA across LLC-PK$_1$ cell monolayers was directional from the basolateral to apical side, and was stimulated markedly by acidification of the apical medium.[11] In the present study, we characterized creatinine transport in renal epithelial cells LLC-PK$_1$ cultured on porous membrane filters.

Methods

Cell Culture: LLC-PK$_1$ cells, obtained from the

Received; January 31, 2005, Accepted; April 7, 2005

To whom correspondence should be addressed: Ken-ichi INUI, Ph.D., *Department of Pharmacy, Kyoto University Hospital, Shogoin, Sakyo-ku, Kyoto 606-8507, Japan. Tel. +81-75-751-3577, Fax. +81-75-751-4207, E-mail: inui@kuhp.kyoto-u.ac.jp*

American Type Culture Collection (ATCC CRL-1392; Rockville, MD, USA), were grown on plastic dishes in Dulbecco's modified Eagle's medium (Sigma-Aldrich, St. Louis, MO, USA), supplemented with 10% fetal bovine serum (Thermo Trace, Victoria, Australia) without antibiotics in an atmosphere of 5% CO_2/95% air at 37°C.[18] For transport experiments, the cells were seeded on microporous membrane filters (3-μm pore, 4.71-cm^2 growth area) inside Transwell® cell culture chambers (Costar, Cambridge, MA, USA) at a density of 5×10^5 cells/cm^2. The cell monolayers were used for transport experiments at 6 days after seeding. In this study, LLC-PK_1 cells between passages 213 and 223 were used.

Uptake Experiments with LLC-PK_1 Cells: The transport of [^{14}C]creatinine and [^{14}C]TEA by LLC-PK_1 cells was measured using cell monolayers grown in Transwell® cell chambers (Costar).[11-13] [^{3}H]D-Mannitol was used to calculate paracellular fluxes and the extracellular trapping of [^{14}C]creatinine and [^{14}C]TEA. The incubation medium for the uptake experiments contained: 145 mM NaCl, 3 mM KCl, 1 mM $CaCl_2$, 0.5 mM $MgCl_2$, 5 mM D-glucose and 5 mM HEPES (pH 7.4). The composition of the high K^+ incubation medium was 3 mM NaCl, 145 mM KCl, 1 mM $CaCl_2$, 0.5 mM $MgCl_2$, 5 mM D-glucose and 5 mM HEPES (pH 7.4). The pH of the medium was adjusted with NaOH or HCl. After removal of the culture medium from both sides of the monolayers, the cells were washed once with 2 mL of incubation medium in each side for the 4.71-cm^2 chamber and then incubated for 10 min at 37°C with 2 mL of the same medium in each side. The medium was replaced with 2 mL of incubation medium containing [^{14}C]creatinine or [^{14}C]TEA in either the apical or basolateral side and the cells were incubated at 37°C. The incubation medium without substrates was added to the opposite side. The medium was immediately aspirated off and the culture inserts were rapidly rinsed twice with 2 mL of ice-cold incubation medium in each side. The cells were solubilized in 0.5 mL of 0.5N NaOH, and then the radioactivity in aliquots was determined by liquid scintillation counting. The protein content of the solubilized cells was determined by the method of Bradford,[14] using a Bio-Rad Protein Assay Kit (Bio-Rad Laboratories, Hercules, CA, USA) with bovine γ-globulin as a standard. For the *cis*-inhibition experiment, the uptake of [^{14}C]creatinine was achieved by adding various concentrations of unlabeled inhibitors to the incubation medium.

Materials: [2-^{14}C]Creatinine hydrochloride (55 mCi/mmol) and [ethyl-1-^{14}C] tetraethylammonium bromide (55 mCi/mmol) were purchased from American Radiolabeled Chemicals (St. Louis, MO, USA). D-[1-^{3}H(N)]Mannitol (17 Ci/mmol) were obtained from PerkinElmer Life Science Products (Boston, MA, USA). Unlabeled creatinine, cimetidine, tetraethylammonium bromide, (±)-chlorpheniramine maleate, quinidine, guanidine hydrochloride, salicylic acid and p-aminohippuric acid were obtained from Nacalai Tesque (Kyoto, Japan). 1-Methyl-4-phenylpyridinium iodide, N^1-methylnicotinamide iodide and probenecid were purchased from Sigma-Aldrich. Trimethoprim was obtained from Wako Pure Chemical Industries (Osaka, Japan). All other compounds used were of the highest purity available.

Statistical Analyses: Data were analyzed statistically with one-way analysis of variance followed by Dunnett's test. P values of less than 0.05 were considered to be significant.

Results

We measured the transepithelial flux and intracellular accumulation of creatinine across LLC-PK_1 cell monolayers grown on porous membrane filters, in comparison with the transport of tetraethylammonium, TEA, a typical organic cation (**Fig. 1**). The basolateral-to-apical transport of [^{14}C]creatinine and [^{14}C]TEA was much greater than the apical-to-basolateral transport, and its rate was nearly constant for up to 60 min (**Figs. 1A and 1C**). The cellular accumulation of [^{14}C]creatinine and [^{14}C]TEA from the basolateral side after the transport experiments for 60 min was 2.0- and 3.6-fold greater than that from the apical side, respectively (**Figs. 1B and 1D**). These results suggested that creatinine was subjected to directional transport across LLC-PK_1 cell monolayers, corresponding to the renal tubular secretion.

Figure 2 shows the time-course and concentration-dependence of the accumulation of [^{14}C]creatinine from the basolateral side of LLC-PK_1 cell monolayers. The accumulation was linear for up to 5 min (**Fig. 2A**). Furthermore, [^{14}C]creatinine accumulation for 5 min was saturated at high concentrations (**Fig. 2B**). After subtracting the nonspecific component of [^{14}C]creatinine accumulation in the presence of 5 mM 1-methyl-4-phenylpyridinium, the mean ± S.E. of the apparent Michaelis constant (K_m) and maximal uptake rate (V_{max}) were obtained from three separate experiments as 13.2 ± 2.8 mM and 13.1 ± 3.1 nmol/mg protein/5 min, respectively. Eadie-Hofstee plots (inset of **Fig. 2B**) for these experiments seemed to be linear, suggesting the involvement of a single transport system.

Next, we examined the effect of membrane potential on the accumulation of [^{14}C]creatinine from the basolateral side. As shown in **Fig. 3**, the accumulation of [^{14}C]creatinine and [^{14}C]TEA from the basolateral side of LLC-PK_1 cell monolayers decreased in the presence of high K^+ (145 mM) buffer, as did that of [^{14}C]TEA. Furthermore, the accumulation of [^{14}C]creatinine and [^{14}C]TEA decreased in the presence of 10 mM

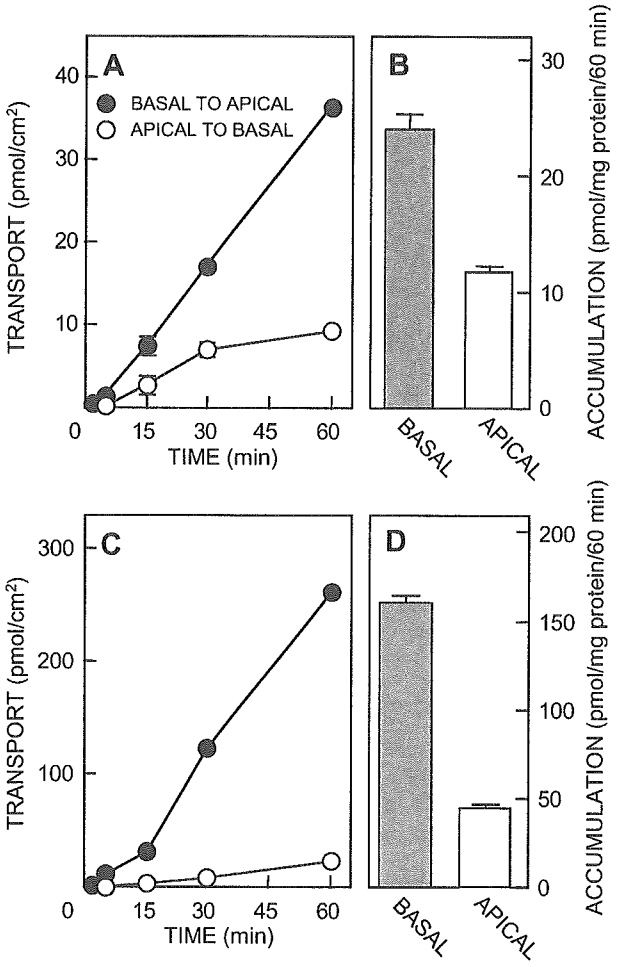

Fig. 1. Transcellular transport and accumulation of [^{14}C]creatinine (A and B) and [^{14}C]TEA (C and D) in LLC-PK$_1$ cell monolayers. LLC-PK$_1$ cells were incubated at 37°C with 5 μM [^{14}C]creatinine or 5 μM [^{14}C]TEA added to the basolateral (closed circle, pH 7.4) or apical (open circle, pH 7.4) side. The radioactivity on the opposite side was periodically measured (A and C). After a 60-min incubation, the radioactivity of solubilized cells was measured (B and D). Each point or column represents the mean ± S.E. for three monolayers from a typical experiment. When error bars are not shown, they are included within the symbols (A and C).

Ba^{2+}, a nonselective K^+ channel blocker.[18]

To investigate further the involvement of organic cation transporters in [^{14}C]creatinine transport in LLC-PK$_1$ cell monolayers, we evaluated the effects of concomitant organic ions (1 mM) added to the basolateral side on the transcellular transport and accumulation of [^{14}C]creatinine. In this experiment, the transport of [^{14}C]creatinine was measured for 15 min to obtain a sufficient amount of radioactivity in the apical chamber. As shown in **Fig. 4**, trimethoprim, cimetidine, quinidine, and 1-methyl-4-phenylpyridinium inhibited both the basolateral-to-apical transport and accumulation of [^{14}C]creatinine. Other organic cations such as TEA, chlorpheniramine, and N^1-methylnicotinamide

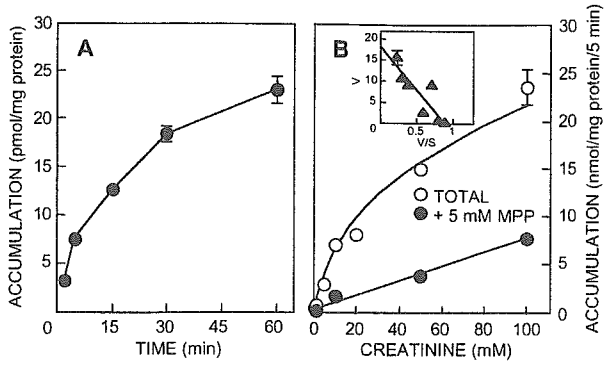

Fig. 2. Time course (A) and concentration-dependence (B) of [^{14}C]creatinine accumulation in LLC-PK$_1$ cell monolayers. *A*; LLC-PK$_1$ cells were incubated for the specified periods at 37°C with 5 μM [^{14}C]creatinine added to the basolateral side. The pHs of both apical and basolateral media were 7.4. Each point represents the mean ± S.E. of three independent experiments. *B*; LLC-PK$_1$ cells were incubated at 37°C for 5 min with the various concentrations of [^{14}C]creatinine indicated in the absence (open circle) or presence (closed circle) of 5 mM 1-methyl-4-phenylpyridinium (MPP) added to the basolateral side. The pHs of both apical and basolateral media were 7.4. Each point represents the mean ± S.E. for three monolayers from a typical experiment. *Inset*: Eadie-Hofstee plots of [^{14}C]creatinine uptake after a correction for nonsaturable components. V, uptake rate (nmol/mg protein/5 min); S, creatinine concentration (mM). When error bars are not shown, they are included within the symbols.

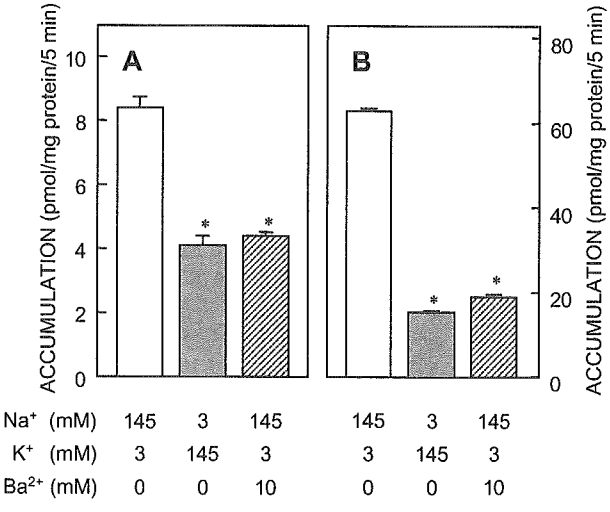

Fig. 3. Effect of membrane potential on uptake of [^{14}C]creatinine (A) and [^{14}C]TEA (B) from the basolateral side in LLC-PK$_1$ cell monolayers. LLC-PK$_1$ cell monolayers were incubated at 37°C for 5 min with incubation medium at the indicated ion concentrations on both sides (pH 7.4) with 5 μM [^{14}C]creatinine (A) or 5 μM [^{14}C]TEA (B) added to the basolateral side. Each column represents the mean ± S.E. for three monolayers from a typical experiment. *, $P<0.05$, significant difference from control using analysis of variance followed by Dunnett's test.

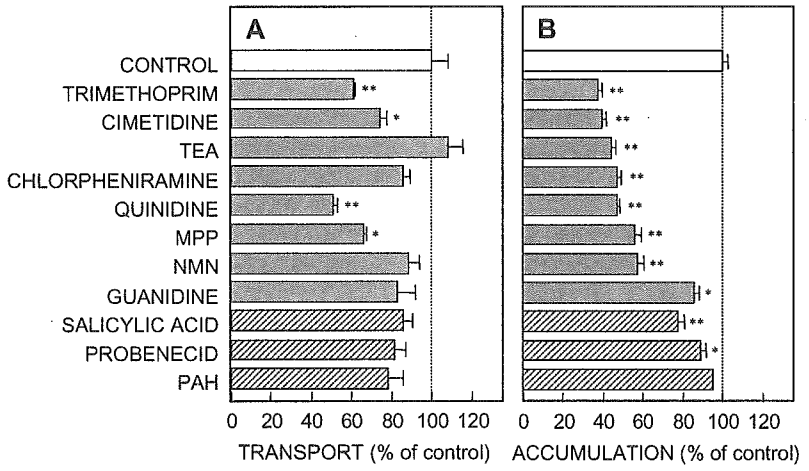

Fig. 4. Effect of organic cations and anions on the transcellular transport (A) and accumulation (B) of [^{14}C]creatinine in LLC-PK$_1$ cell monolayers. LLC-PK$_1$ cell monolayers were incubated at 37°C for 15 min with 5 μM [^{14}C]creatinine added to the basolateral side in the absence (control) or presence of cationic or anionic compounds (1 mM) on the basolateral side. The pHs of both basolateral and apical media were 7.4. MPP, 1-methyl-4-phenylpyridinium; NMN, N^1-methylnicotinamide; PAH, *p*-aminohippuric acid. Each column represents the mean ± S.E. for three monolayers from a typical experiment. *, $P<0.05$; **, $P<0.01$, significant difference from control using analysis of variance followed by Dunnett's test.

also inhibited significantly the accumulation of [^{14}C]creatinine from the basolateral side (**Fig. 4B**). Furthermore, guanidine, salicylic acid, and probenecid slightly inhibited the accumulation of [^{14}C]creatinine from the basolateral side (**Fig. 4B**). In contrast, *p*-aminohippuric acid had little inhibitory effect on both the transcellular transport (**Fig. 4A**) and accumulation (**Fig. 4B**).

Finally, we examined the effect of apical pH on the transcellular transport and accumulation of [^{14}C]creatinine. Both the transcellular transport (**Fig. 5A**) and accumulation (**Fig. 5B**) of [^{14}C]creatinine were mostly independent of the apical pH. In contrast, the transcellular transport of [^{14}C]TEA increased markedly with the acidification of the apical medium (**Fig. 5C**), as demonstrated by us.[11] Consistent with the increased extrusion of [^{14}C]TEA from the cells across apical membranes, the accumulation of [^{14}C]TEA decreased (**Fig. 5D**).

Discussion

Although organic ion transporters have been implicated in the tubular secretion of creatinine,[15,16] the characteristics of tubular secretion of creatinine have not been clarified. In the present study, we found that the transport of creatinine across LLC-PK$_1$ cell monolayers was directional from the basolateral to apical side (**Fig. 1**), and was markedly reduced in the presence of organic cations (**Fig. 4**), suggesting the involvement of organic cation transporters in the transcellular transport of creatinine. This is the first report to demonstrate the transcellular transport of creatinine *via* organic cation transport systems.

Several organic cation transporters (OCTs) have been identified.[5] hOCT2 is the dominant organic cation transporter in the human kidney,[17] and is driven by differences in membrane potential, mediating the basolateral uptake of organic cations into the renal epithelial cells. Recently, we demonstrated that creatinine was specifically transported by hOCT2, but not hOCT1 in the cDNA transfected HEK293 cells.[18] In the present study, the basolateral uptake of creatinine was dependent on the inside-negative membrane potential, being consistent with our previous findings. In addition, the apparent K_m value of the basolateral uptake of creatinine in LLC-PK$_1$ cells (13.2 ± 2.8 mM, **Fig. 2B**) was comparable to that in the hOCT2-expressing HEK293 cells (4.0 ± 0.3 mM).[18] Furthermore, the ability of various organic ions to inhibit the cellular accumulation of creatinine (**Fig. 4**) suggested that the creatinine uptake in LLC-PK$_1$ cells is mediated by an OCT-like transporter expressed at the basolateral membrane.

Acidification of the apical medium did not stimulate the elimination of creatinine from the cells, in contrast to the marked stimulation of apical excretion of TEA (**Fig. 5**). These results suggested that the contribution of the H^+/organic cation antiporter to the apical extrusion of creatinine is limited. Provided that the volume of LLC-PK$_1$ cells is 3.4 μL/mg protein,[19] the intracellular concentration of [^{14}C]creatinine after a 60-min incubation reached 7.4 μM (**Fig. 1B**), which was about 1.5-fold the extracellular concentration of [^{14}C]creatinine (5 μM). Taking into consideration that the accumulation of TEA was highly concentrative, i.e. 10-fold higher than that of extracellular [^{14}C]TEA (**Fig. 1D**), the transport of creatinine both at apical and basolateral

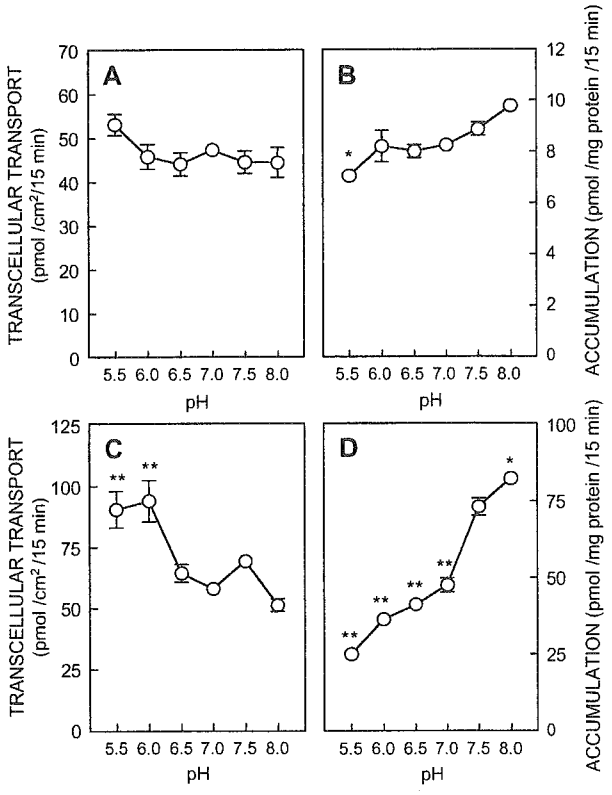

Fig. 5. Effect of apical pH on transcellular transport and accumulation of [^{14}C]creatinine (A and B) and [^{14}C]TEA (C and D) in LLC-PK$_1$ cell monolayers. LLC-PK$_1$ cell monolayers were incubated at 37°C for 15 min with 5 μM [^{14}C]creatinine or [^{14}C]TEA added to the basolateral side and apical media of various pH (5.5-8.0). The pH of the basolateral medium was 7.4. The radioactivity in the apical medium (A and C) and solubilized cells (B and D) was measured after incubation. Each point represents the mean ± S.E. for three monolayers from a typical experiment. *, $P<0.05$; **, $P<0.01$, significant difference from the value at pH 7.4 using analysis of variance followed by Dunnett's test. When error bars are not shown, they are included within the symbols.

membranes should be comparable with that of TEA.

In the present study, concomitant administration of cimetidine and trimethoprim significantly inhibited the creatinine transport across LLC-PK$_1$ cell monolayers (**Fig. 4**). It is reported that oral cimetidine administration improves the preciseness of GFR estimation due to the inhibition of tubular creatinine secretion in patients with renal diseases and renal transplant recipients.[16,20] In another study by Berglund *et al.*,[15] the serum creatinine level was elevated by a twice-daily administration of 160 mg of trimethoprim plus 800 mg of sulfamethoxazole through inhibition of the tubular secretion of creatinine. It is reported that a single oral dose of 200 mg of cimetidine to patients with normal renal function gave C_{max} values of between 2.3 μM and 6.8 μM,[21] which is lower than the IC_{50} value of cimetidine for the uptake of creatinine by hOCT2 (27 ± 6 μM).[18] On the other hand, the IC_{50} value of trimethoprim for the uptake of creatinine by hOCT2 (21 ± 2 μM) was marginal in view of the hOCT2-mediated transport of creatinine at therapeutic concentrations of trimethoprim.[18] Considering that a higher dose of cimetidine (800 mg daily) is used for the treatment of gastric and duodenal ulcers and reflux esophagitis and the systemic clearance of cimetidine and trimethoprim is delayed in patients with decreased renal functions. Concomitant administration of these drugs would interfere in part with the tubular secretion of creatinine via hOCT2 and increase the serum creatinine level.

In conclusion, we have demonstrated for the first time that transport of creatinine across renal epithelial cells was directional from the basolateral to apical side. These observations are relevant for understanding the molecular mechanisms underlying the tubular secretion of creatinine.

Acknowledgements: This work was supported in part by a grant-in-aid for Comprehensive Research on Aging and Health from the Ministry of Health, Labor and Welfare of Japan, a grant-in-aid for Scientific Research from the Ministry of Education, Science, Culture and Sports of Japan, and by the 21st Century COE program "Knowledge Information Infrastructure for Genome Science".

References

1) Kasiske, B. L. and Keane, W. F.: Laboratory assessment of renal disease: clearance, urinalysis, and renal biopsy. in Brenner, B. M. (ed): *The kidney*. W. B. Saunders, Philadelphia, PA, USA, 2000, pp. 1129-1170.
2) Sjostrom, P. A., Odlind, B. G. and Wolgast, M.: Extensive tubular secretion and reabsorption of creatinine in humans. *Scand. J. Urol. Nephrol.*, **22**: 129-131 (1988).
3) Shemesh, O., Golbetz, H., Kriss, J. P. and Myers, B. D.: Limitations of creatinine as a filtration marker in glomerulopathic patients. *Kidney Int.*, **28**: 830-838 (1985).
4) Inui, K. and Okuda, M.: Cellular and molecular mechanisms of renal tubular secretion of organic anions and cations. *Clin. Exper. Nephrol.*, **2**: 100-108 (1998).
5) Inui, K., Masuda, S. and Saito, H.: Cellular and molecular aspects of drug transport in the kidney. *Kidney Int.*, **58**: 944-958 (2000).
6) Koepsell, H.: Organic cation transporters in intestine, kidney, liver, and brain. *Annu. Rev. Physiol.*, **60**: 243-266 (1998).
7) Pritchard, J. B. and Miller, D. S.: Mechanisms mediating renal secretion of organic anions and cations. *Physiol. Rev.*, **73**: 765-796 (1993).
8) Takano, M., Inui, K., Okano, T., Saito, H. and Hori, R.: Carrier-mediated transport systems of tetraethylammonium in rat renal brush-border and basolateral membrane vesicles. *Biochim. Biophys. Acta.*, **773**: 113-124 (1984).

9) Wright, S. H.: Transport of N^1-methylnicotinamide across brush border membrane vesicles from rabbit kidney. *Am. J. Physiol.*, **249**: F903-F911 (1985).
10) Inui, K., Saito, H. and Hori, R.: H^+-gradient-dependent active transport of tetraethylammonium cation in apical-membrane vesicles isolated from kidney epithelial cell line LLC-PK_1. *Biochem. J.*, **227**: 199-203 (1985).
11) Saito, H., Yamamoto, M., Inui, K. and Hori, R.: Transcellular transport of organic cation across monolayers of kidney epithelial cell line LLC-PK_1. *Am. J. Physiol.*, **262**: C59-C66 (1992).
12) Ohtomo, T., Saito, H., Inotsume, N., Yasuhara, M. and Inui, K.: Transport of levofloxacin in a kidney epithelial cell line, LLC-PK_1: interaction with organic cation transporters in apical and basolateral membranes. *J. Pharmacol. Exp. Ther.*, **276**: 1143-1148 (1996).
13) Takami, K., Saito, H., Okuda, M., Takano, M. and Inui, K.: Distinct characteristics of transcellular transport between nicotine and tetraethylammonium in LLC-PK_1 cells. *J. Pharmacol. Exp. Ther.*, **286**: 676-680 (1998).
14) Bradford, M. M.: A rapid and sensitive method for the quantitation of microgram quantities of protein utilizing the principle of protein-dye binding. *Anal. Biochem.*, **72**: 248-254 (1976).
15) Berglund, F., Killander, J. and Pompeius, R.: Effect of trimethoprim-sulfamethoxazole on the renal excretion of creatinine in man. *J. Urol.*, **114**: 802-808 (1975).
16) van Acker, B. A. C., Koomen, G. C. M., Koopman, M. G., de Waart, D. R. and Arisz, L.: Creatinine clearance during cimetidine administration for measurement of glomerular filtration rate. *Lancet*, **340**: 1326-1329 (1992).
17) Motohashi, H., Sakurai, Y., Saito, H., Masuda, S., Urakami, Y., Goto, M., Fukatsu, A., Ogawa, O. and Inui, K.: Gene expression levels and immunolocalization of organic ion transporters in the human kidney. *J. Am. Soc. Nephrol.*, **13**: 866-874 (2002).
18) Urakami, Y., Kimura, N., Okuda, M. and Inui, K.: Creatinine transport by basolateral organic cation transporter hOCT2 in the human kidney. *Pharm. Res.*, **21**: 976-981 (2004).
19) Tomita, Y., Otsuki, Y., Hashimoto, Y. and Inui, K.: Kinetic analysis of tetraethylammonium transport in the kidney epithelial cell line, LLC-PK_1. *Pharm. Res.*, **14**: 1236-1240 (1997).
20) Kemperman, F. A., Surachno, J., Krediet, R. T. and Arisz, L.: Cimetidine improves prediction of the glomerular filtration rate by the Cockcroft-Gault formula in renal transplant recipients. *Transplantation*, **73**: 770-774 (2002).
21) Larsson, R., Bodemar, G. and Norlander, B.: Oral absorption of cimetidine and its clearance in patients with renal failure. *Eur. J. Clin. Pharmacol.*, **15**: 153-157 (1979).

Am J Physiol Gastrointest Liver Physiol 289: G471–G477, 2005.
First published May 19, 2005; doi:10.1152/ajpgi.00025.2005.

Characterization of the human peptide transporter PEPT1 promoter: Sp1 functions as a basal transcriptional regulator of human PEPT1

Jin Shimakura, Tomohiro Terada, Toshiya Katsura, and Ken-Ichi Inui

Department of Pharmacy, Kyoto University Hospital, Faculty of Medicine, Kyoto University, Sakyo-ku, Japan

Submitted 24 January 2005; accepted in final form 12 May 2005

Shimakura, Jin, Tomohiro Terada, Toshiya Katsura, and Ken-Ichi Inui. Characterization of the human peptide transporter PEPT1 promoter: Sp1 functions as a basal transcriptional regulator of human PEPT1. *Am J Physiol Gastrointest Liver Physiol* 289: G471–G477, 2005. First published May 19, 2005; doi:10.1152/ajpgi.00025.2005.—H^+-coupled peptide transporter 1 (PEPT1, SLC15A1) localized at the brush-border membranes of intestinal epithelial cells plays an important role in the intestinal absorption of small peptides and a variety of peptidemimetic drugs. PEPT1 is regulated by various factors, including hormones, dietary conditions, some pharmaceutics, and diurnal rhythm. But there is little information about the transcriptional regulation of PEPT1. In the present study, therefore, we cloned the human (h)PEPT1 promoter region and examined its promoter activity using a human intestinal cell line, Caco-2. Deletion analysis of the hPEPT1 promoter suggested that the region spanning −172 to −35 bp was essential for basal transcriptional activity. This region lacked a TATA-box but contained some GC-rich sites that supposedly bind with the transcription factor Sp1. Mutational analysis revealed that three of these putative Sp1 sites contributed to the transcriptional activity. EMSA showed that Sp1 bound to two GC-rich sites. Furthermore, inhibition of Sp1 binding by mithramycin A treatment significantly reduced the transcriptional activity. Finally, overexpression of Sp1 increased the transcriptional activity in a dose-dependent manner. This study reports the first characterization of the hPEPT1 promoter and shows the significant role of Sp1 in the basal transcriptional regulation of hPEPT1.

Caco-2; SLC15A1; small intestine

DIETARY PROTEINS ARE DEGRADATED into a mixture of free amino acids and small peptides. Cellular uptake of di- and tripeptides is mediated by H^+-coupled peptide transporter 1 (PEPT1, SLC15A1) located at the brush-border membranes of intestinal epithelial cells (8). Because of its broad substrate specificity, PEPT1 can accept several peptidelike drugs such as oral β-lactam antibiotics, the anticancer agent bestatin, and angiotensin-converting enzyme inhibitors (28). Thus PEPT1 plays important roles not only as a nutrient transporter but also as a drug transporter. It has been reported that intestinal PEPT1 is regulated by various factors (1), including hormones [insulin (11), thyroid hormone (2)], epidermal growth factor (18), cytokine (interferon-γ) (7), dietary conditions (17, 24), some pharmacological agents (3, 10), and diurnal rhythm (19). Although the elucidation of these regulatory mechanisms is quite important for nutritional therapy for absorptive disorders and for the efficient oral delivery of peptidelike drugs in a clinical situation, studies that address this point are limited. Shiraga et al. (24) has cloned the 5′-flanking region of rat PEPT1 and revealed that the rat PEPT1 promoter was transcriptionally regulated by some amino acids via the amino acid responsible element. In the mouse PEPT1 promoter, a functional promoter analysis demonstrated that essential promoter/enhancer sites were present within 1140 bp upstream of the transcription start site (9). Nevertheless, *cis* elements and/or *trans* factors, which are critical for basal transcriptional regulation, have not been identified in these studies. As for human (h)PEPT1, a computational sequence analysis but not a functional analysis has been conducted (29).

In the present study, to fully understand the transcriptional regulation of PEPT1, we cloned the 5′-flanking region of the hPEPT1 gene and identified the minimal region and *cis*-regulatory elements required for the basal hPEPT1 promoter activity. In addition, the results provide evidence for the involvement of Sp1 in the regulation of basal promoter activity.

MATERIALS AND METHODS

Materials. γ-[^{32}P]ATP was obtained from Amersham Biosciences (Buckinghamshire, UK). Anti-human Sp1 was purchased from Upstate (Charlottesville, VA). Restriction enzymes were from New England BioLabs (Beverly, MA). Mithramycin A was purchased from Sigma-Aldrich (St. Louis, MO). CMV-Sp1 plasmid was kindly provided by Dr. Robert Tjian (University of California, Berkeley, CA). All other chemicals used were of the highest purity available.

Cloning of the 5′-regulatory region of hPEPT1 gene. The 2940-bp flanking region upstream of the transcription start site, which was indicated in the literature (29), was cloned using primers (hPT1proSacI-F, hPT1proXhoI-R) shown in Table 1 and human genomic DNA (Promega, Madison, WI). The primers were designed based on the genomic sequence deposited in the literature (29). The PCR conditions were denaturing at 95°C for 5 min, followed by 30 cycles of denaturing at 95°C for 1 min, annealing at 60°C for 1 min, and extension at 72°C for 4 min, before a final extension at 72°C for 10 min. The PCR product was isolated by electrophoresis and subcloned into the firefly luciferase reporter vector, pGL3-Basic (Promega), at *Sac*I and *Xho*I sites. This full-length reporter plasmid is hereafter referred to as −2940/+60.

Preparation of deletion reporter constructs. The 5′-deleted constructs (−1111/+60, −960/+60, −401/+60, −247/+60, −172/+60, −89/+60, −21/+60 constructs) were generated by digestion of the −2940/+60 construct with *Hin*dIII and each of the following enzymes: *Nhe*I, *Kpn*I, *Psh*AI, *Pvu*II, *Apa*I, *Xma*I, and *Aat*II, respectively. The ends were blunted with T4 DNA polymerase and then self-ligated. The −35/+60 construct was generated by PCR with primers containing a *Sac*I site and *Xho*I site (Table 1). The site-directed mutations in putative Sp1-binding sites were introduced into the −172/+60 construct with a Quik Change XL site-directed mutagenesis kit (Stratagene, La Jolla, CA) with the primers listed in Table 1. The nucleotide sequences of these deleted or mutated constructs were

Address for reprint requests and other correspondence: Ken-ichi Inui, Dept. of Pharmacy, Kyoto Univ. Hospital, Sakyo-ku, Kyoto 606-8507, Japan (e-mail: inui@kuhp.kyoto-u.ac.jp).

The costs of publication of this article were defrayed in part by the payment of page charges. The article must therefore be hereby marked "*advertisement*" in accordance with 18 U.S.C. Section 1734 solely to indicate this fact.

Table 1. *Oligonucleotide sequences of primers*

Name	Sequence (5′-3′)	Position
Primers for cloning of the hPEPT1 promoter		
hPEPT1proSacI-F	AGGAGCTCTTTCTCCCTAGGCACCACAGT	−2940 to −2920
hPEPT1proXhoI-R	AGCTCGAGCCATGGCGGCGGCTCCCAGGG	+60 to +40
Primers for the −35/+60 deletion construct		
hPEPT1pro-35SacI-F	AGGAGCTCCGGGGCCGGGCCTGGA	−35 to −20
hPEPT1proXhoI-R	AGCTCGAGCCATGGCGGCGGCTCCCAGGG	+60 to +40
Primers for the site-directed mutagenesis		
Mut A-F	GGTGGAGCCGGCGAACCCAACTCGCAGAGCTGGG	−85 to −52
Mut A-R	CCCAGCTCTGCGAGTTGGGTTCGCCGGCTCCACC	−85 to −52
Mut B-F	CACCGCCCCCCGAATGGATCCGGCGGCCCCG	−97 to −67
Mut B-R	CGGGGCCGCCGGATCCATTCGGGGGCGGTG	−97 to −67
Mut C-F	CTCCCCGCAGCACCGAACTCCGGGTGGAG	−107 to −79
Mut C-R	CTCCACCCGGAGTTCGGTGCTGCGGGGAG	−107 to −79
Mut D-F	CACCCGCACCTGAACCAAGGCTGGTGTCCACGCGC	−167 to −133
Mut D-R	GCGCGTGGACACCAGCCTTGGTTCAGGTGCGGGTG	−167 to −133
Oligonucleotide for EMSA		
Probe(−77/−54)-F1	CGGCGGCCCCGCCTCGCAGAGCTG	−77 to −54
Probe(−77/−54)-R1	CAGCTCTGCGAGGCGGGGCCGCCG	−77 to −54
Mut A-F1	CGGCGAACCCAACTCGCAGAGCTG	−77 to −54
Mut A-R1	CAGCTCTGCGAGTTGGGTTCGCCG	−77 to −54
Probe(−102/−75)-F1	CGCAGCACCGCCCCCCGGGTGGAGCCGG	−102 to −75
Probe(−102/−75)-R1	CCGGCTCCACCCGGGGGGCGGTGCTGCG	−102 to −75
Mut B-F1	CGCAGCACCGCCCCCCGAATGGATCCGG	−102 to −75
Mut B-R1	CCGGATCCATTCGGGGGGCGGTGCTGCG	−102 to −75
Mut C-F1	CGCAGCACCGAACTCCGGGTGGAGCCGG	−102 to −75
Mut C-R1	CCGGCTCCACCCGGAGTTCGGTGCTGCG	−102 to −75
Sp1-consensus-F1	ATTCGATCGGGGCGGGGCGAGC	
Sp1-consensus-R1	GCTCGCCCCGCCCCGATCGAAT	

*Sac*I and *Xho*I sites are underlined. Mutations introduced into the oligonucleotides are shown in bold. hPEPT1, human peptide transporter; Mut, mutation.

confirmed using a multicapillary DNA sequencer RISA384 system (Shimadzu, Kyoto, Japan).

Cell culture, transfection, and reporter gene assay. Caco-2 cells were obtained from the American Type Culture Collection (ATCC CRL-1392) and maintained in Dulbecco's modified Eagle's medium supplemented with 10% fetal bovine serum and 1% nonessential amino acids. Caco-2 cells were plated into 24-well plates (3×10^5 cells/well) and transfected the following day with the reporter constructs and 2.5 ng of the *Renilla reniformis* vector pRL-TK (Promega) using Lipofectamine 2000 (Invitrogen Japan KK, Tokyo, Japan) according to the manufacturer's recommendation. The medium was changed after 24 h. The firefly and *Renilla* activities were determined 48 h after the transfection using a dual luciferase assay kit (Promega) and a LB940 luminometer (Berthold, Bad Wildbad, Germany). The firefly activity was normalized to *Renilla* activity except for the CMV-Sp1 overexpression, which significantly stimulated the *Renilla* activity. For the inhibition experiment with mithramycin A, Caco-2 cells were treated with 50, 100, and 250 nM of mithramycin A at the time of transfection of the reporter constructs.

EMSA. Nuclear extract (NE) was prepared from Caco-2 cells grown in 60-mm culture dishes for 16 days. Cells were scraped off, suspended in 0.5 ml PBS, and centrifuged at 4°C and 1,500 *g* for 5 min. The cells were resuspended in 0.4 ml of a low-salt buffer [in mM: 10 HEPES (pH 7.9), 10 KCl, 0.1 EDTA, 0.1 EGTA, 1 DTT, and 0.5 PMSF, with 1% protease inhibitor cocktail (Nacalai tesque, Kyoto, Japan)] and incubated on ice for 15 min. After 50 μl of Nonidet P-40 were added, the tube was vigorously vortexed for 10 s and centrifuged at 4°C and 20,000 *g* for 5 min. The supernatant was removed and the nuclear pellet was resuspended in 50 μl of a high-salt buffer [in mM: 20 HEPES (pH 7.9), 400 NaCl, 1 EDTA, 1 EGTA, 1 DTT, and 1 PMSF, with 1% protease inhibitor cocktail], and the tube was vigorously shaken (250 rpm) at 4°C for 30 min. The tube was centrifuged at 4°C and 20,000 *g* for 5 min, and the supernatant was recovered.

The probes shown in Table 1 were prepared by annealing complementary sense and antisense oligonucleotides, followed by end-labeling with γ-[^{32}P]ATP using T4 polynucleotide kinase (Takara Bio, Otsu, Japan) and purification through a Sephadex G-25 column (Amersham Biosciences). EMSAs were performed according to the instructions for the Gel shift assay system (Promega). The binding mixture consisted of 1 μg Caco-2 nuclear extract, 0.5 μg poly(dI-dC), and unlabeled competitor probes in buffer solution containing (in mM) 10 Tris·HCl (pH 7.5), 50 NaCl, 1 $MgCl_2$, 0.5 EDTA, and 0.5 DTT, with 4% glycerol. After preincubation at room temperature for 10 min, labeled probes (~0.4 ng) were added and the binding mixture was incubated for a further 20 min. For supershift assays, 1 μg Sp1 antibody was added 10 min before the addition of the labeled probes. The volume of the binding mixture was 10 μl throughout the experiment. The DNA-protein complex was then separated on a 4% polyacrylamide gel at room temperature in 0.5 × Tris-borate-EDTA buffer. The gels were dried and exposed to X-ray film for autoradiography.

Data analysis. The results were expressed relative to the pGL3-Basic vector set at 1 except for the Sp1 overexpression experiment and represent the means ± SE of three replicates. Two or three experiments were conducted, and representative results were shown. In the mutational, Sp1 overexpression and inhibition experiments, statistical analysis was performed with the one-way ANOVA followed by Scheffé's *F*-post hoc testing.

RESULTS

Determination of minimal hPEPT1 promoter. To determine the minimal region required for basal activity of the promoter, a series of deletion constructs was transfected into Caco-2 cells and luciferase activity was measured (Fig. 1). The transfection with the longest reporter constructs (−2940/+60) resulted in a three- to fourfold-increase in luciferase activity compared with

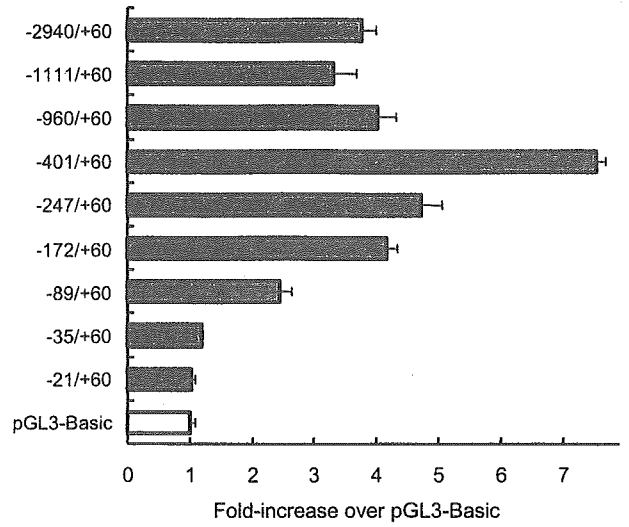

Fig. 1. Identification of transcriptional activity and deletion analysis of the human peptide transporter (hPEPT1) promoter in Caco-2 cells. A series of deleted promoter constructs [equimolar amounts of the −2940/+60 construct (500 ng)] were transfected into Caco-2 cells for luciferase assays. Firefly luciferase activity was normalized to *Renilla* luciferase activity. Data are reported as the relative fold increase compared with pGL3-Basic vector and represent the means ± SE of 3 replicates.

pGL3-Basic. The −1111/+60 construct reduced luciferase activity, suggesting the existence of some positive regulatory sites between −2940 and −1111. Deletion of the sequence from nucleotides −1111 to −960 and further deletion from −960 to −401 resulted in an increase in promoter activity, suggesting the presence of repressive elements in these regions. The −401/+60 construct had the strongest promoter activity, i.e., a sixfold increase in luciferase activity compared with pGL3-Basic. Serial 5′-deletions of the construct from −401 to −247, −172, −89, and −35 gradually reduced the activity, which was completely abolished with the −35/+60 construct. Thus the elements important for the basal promoter activity were shown to be located between −401 and −35. We considered the region between −172 and −35 to be the minimal promoter, because the −172/+60 construct retained fourfold greater activity than pGL3-Basic, which is almost the same level of activity as the longest construct, −2940/+60.

We performed a computational sequence analysis on the −401/−1 region of the hPEPT1 promoter, which had the strongest activity, using TFSEARCH at www.cbrc.jp/research/db/TFSEARCH.html (Fig. 2). This analysis revealed that the region proximal to the transcription start site lacks canonical TATA or CAAT boxes. Instead, several GC-rich sites were observed, suggesting a possible contribution of Sp1 to the transcriptional regulation of hPEPT1. This promoter region also had putative binding sites for AP-1, CREB, myeloid zinc finger 1, and caudal-related homeobox transcription factor Cdx A. Considering that the minimal regulatory elements are located downstream of −172, we subsequently focused on these putative Sp1-binding sites between −172 and −35.

Mutagenesis of the Sp1 sites. The putative Sp1-binding sites located between −172 and −35 were designated Sp-A, Sp-B, Sp-C, and Sp-D, as shown in Fig. 3*A*. To determine whether these sites were important for hPEPT1 promoter activity, mutations in these sites (*mut A*, *mut B*, *mut C*, and *mut D*, respectively) were introduced in the −172/+60 construct (Fig. 3*A*) and transfected into Caco-2 cells. As shown in Fig. 3*B*, *mut A* reduced the luciferase activity to one-third of the wild-type (WT) level. The luciferase activity was also markedly reduced by introducing *mut B* or *C*, whereas little effect was observed with *mut D*. These results suggest that the Sp-A, -B, and -C sites play an important role in regulating the hPEPT1 promoter activity.

EMSA. Next, we performed an EMSA using two oligonucleotide probes, *probe −77/−54* and *probe −102/−75*, and nuclear extract from Caco-2 cells to determine directly whether Sp1 binds to the promoter. *Probe −77/−54* formed three DNA-protein complexes, that is, complex I, II, and III, with the

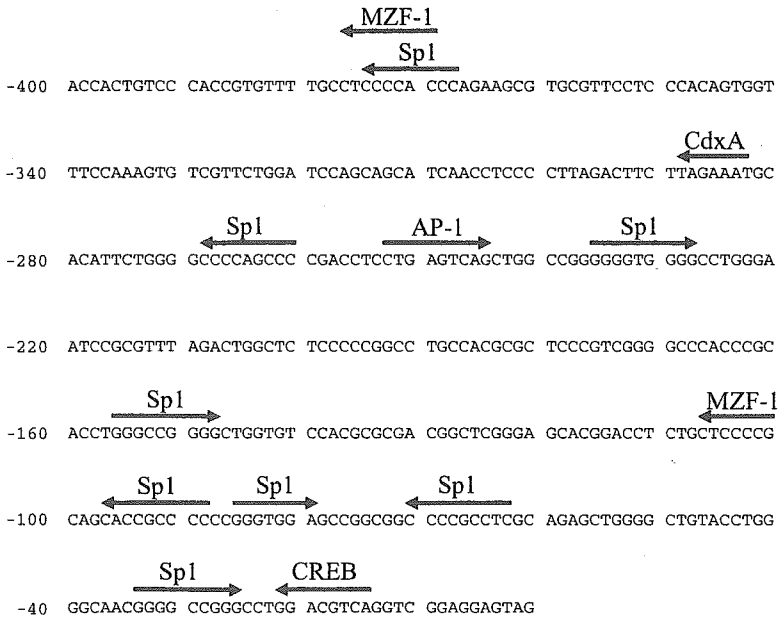

Fig. 2. Nucleotides sequence of the promoter region (−401 to −1) that had the highest basal activity. Numbering is relative to the transcription start site. The putative binding sites for the transcription factors are indicated on the sequence (the arrows indicate the direction). MZF-1, myeloid zinc finger 1.

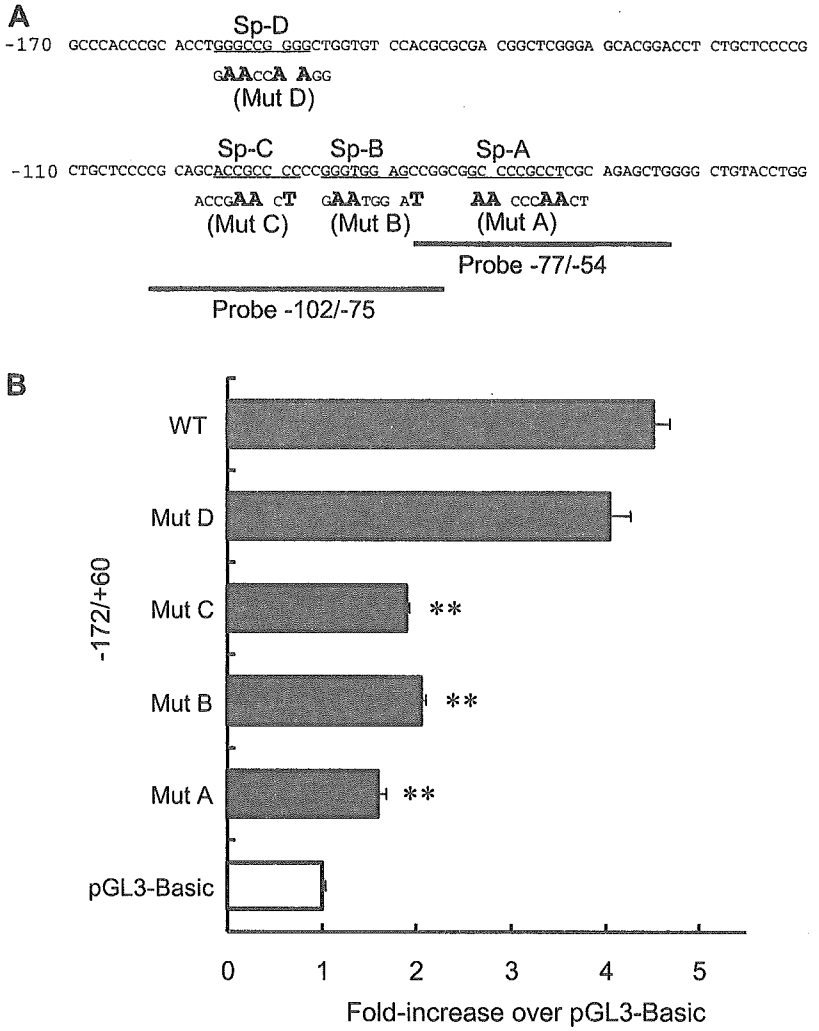

Fig. 3. Mutational analysis of the putative Sp1-binding elements of the hPEPT1 promoter. *A*: the nucleotide sequence of the promoter region of −170 to −41 is shown with the putative Sp1-binding elements (Sp-A, Sp-B, Sp-C, and Sp-D, underlined). Site-directed mutations that destroy Sp1-binding elements were introduced individually and designated *mut A*, *mut B*, *mut C*, and *mut D*. The nucleotides altered for mutational analysis are shown in bold under the wild-type (WT) sequence. The regions used for oligonucleotide probes for EMSA are also indicated. *B*: the mutated −172/+60 constructs (500 ng) were transiently expressed in Caco-2 cells for luciferase assays. Firefly luciferase activity was normalized to *Renilla* luciferase activity. Data are reported as the relative fold increase compared with pGL3-Basic vector and represent the means ± SE of 3 replicates. **Significantly different from WT ($P < 0.01$).

nuclear extract, whereas no complex was formed in the absence of nuclear extract (Fig. 4, *lanes 1* and *2*). The formation of all three complexes was completely competed away by the addition of an excess amount of unlabeled WT oligonucleotide but not by the *mut A* oligonucleotide (Fig. 4, *lanes 3* and *4*), suggesting that all these complexes bind to the Sp-A site. Moreover, Sp1 oligonucleotide competed the formation of complex I and II (Fig. 4, *lane 5*), further suggesting the identity of these factors as Sp1-like proteins. Sp1 appeared to exist in complex I because of the reduction of corresponding band and formation of supershifted band on incubation with anti-Sp1 antibody (Fig. 4, *lane 6*).

Probe −102/−75 formed three DNA-protein complexes (complexes IV, V, and VI) with the nuclear extract, whereas no complex was formed in the absence of nuclear extract (Fig. 4, *lanes 7* and *8*). The formation of the complex IV was completely diminished by the addition of an excess amount of unlabeled WT or *mut B* oligonucleotide but not by *mut C* oligonucleotide (Fig. 4, *lanes 9–11*). These results suggest that Sp-C is a more important region because the *mut B* oligonucleotide retains an intact Sp-C site, whereas the *mut C* oligonucleotide retains an intact Sp-B site. Complex IV was also competed by the addition of Sp1 consensus oligonucleotide and, most importantly, formed a supershifted band on incubation with anti-Sp1 antibody (Fig. 4, *lanes 12* and *13*). Complex V was so faint that its nature was not clear. Although complex VI was clearly detectable when the probe was incubated with nuclear extract only, moderate bands were also observed in every competitor used. This complex VI might be nonspecific, because there was no difference in the intensity of the bands between each competitor.

Inhibition of Sp1-binding by Sp1-specific chemical inhibitor mithramycin A. Mithramycin A is known to bind to the GC box and inhibit Sp1-binding (6, 21). The effect of mithramycin A on the hPEPT1 promoter activity was investigated with the −401/+60 construct in Caco-2 cells (Fig. 5). Treatment with mithramycin A led to a significant decrease in the promoter activity in a dose-dependent manner.

Transactivation of promoter activity by Sp1 overexpression. Finally, we investigated the effect of Sp1 overexpression on the hPEPT1 promoter activity (Fig. 6). The −401/+60 construct was cotransfected into Caco-2 cells with the CMV-Sp1 expression vector. The luciferase activity showed a dose-dependent increase on cotransfection of CMV-Sp1, providing direct evidence that Sp1 enhanced the promoter activity.

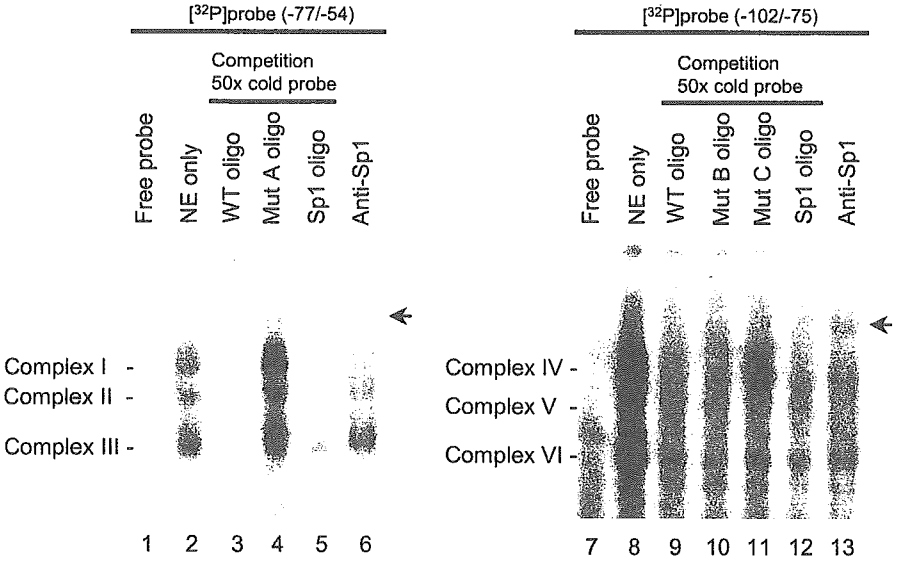

Fig. 4. EMSA of Caco-2 nuclear proteins binding to the probes containing putative Sp1-binding elements. Nuclear extract from Caco-2 cells was incubated with the ^{32}P-labeled oligonucleotide probes (*probe −77/−54* and *probe −102/−75*) alone (*lanes 2* and *8*) or in the presence of excess unlabeled WT oligonucleotide (*lanes 3* and *9*), mutated oligonucleotide (*lanes 4*, *10*, and *11*), Sp1 consensus oligonucleotide (*lanes 5* and *12*), and anti-Sp1 antibody (*lanes 6* and *13*). In *lanes 1* and *7*, nuclear extract was not added. Arrows indicate the supershifted complexes.

DISCUSSION

In the present study, we cloned the 5′-flanking region of the hPEPT1 gene and investigated its transcriptional regulation. When subcloned into a luciferase vector and transfected into Caco-2 cells, the 5′-flanking region showed considerable promoter activity. We used Caco-2 cells because a significant amount of hPEPT1 is expressed constitutively in these cells (2), and the transcription factors and/or cofactors required for the expression exist intrinsically in these cells. In the deletion analysis, the promoter activity was highest with the −401/+60 region, and the minimal promoter was considered to be located in the −172/−35 region. Computational analysis showed the lack of a TATA box and a CAAT box near the transcription start site but the presence of several GC-rich regions. This feature was similar to the mouse PEPT1 promoter, in which a TATA box was not located near the transcription start site, whereas some GC-rich elements were located in the proximal region (9). In such a TATA-less promoter, Sp1 binds to the GC-rich region and this Sp1 site has been shown to be responsible for recruiting TATA-binding protein (20) and fixing the transcription start site (5). Furthermore, the promoter activity is enhanced if multiple Sp1-binding sites exist (14). Thus Sp1 is speculated to play a significant role as a basal

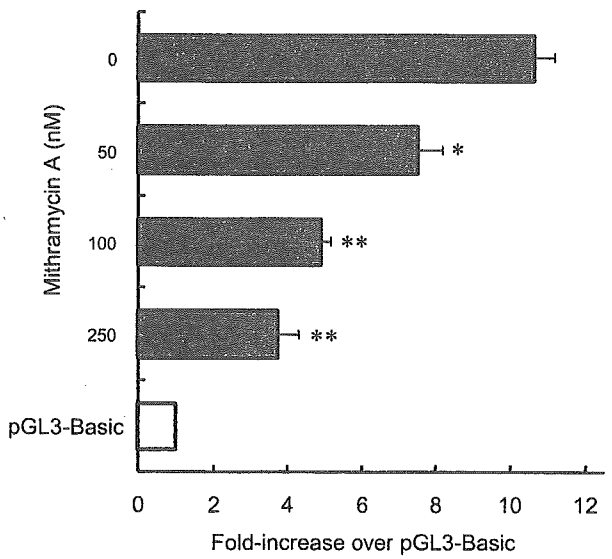

Fig. 5. Inhibition of the hPEPT1 transcriptional activity by mithramycin A. Caco-2 cells were transiently transfected with the −401/+60 construct. Mithramycin A was added to the cells 2 times, just after transfection and after the medium change at 24 h. Firefly luciferase activity was normalized to *Renilla* luciferase activity. Data are reported as the relative fold increase compared with pGL3-Basic vector and represent the means ± SE of 3 replicates. Symbols show significant difference from control (without mithramycin A; $^*P < 0.05$ and $^{**}P < 0.01$).

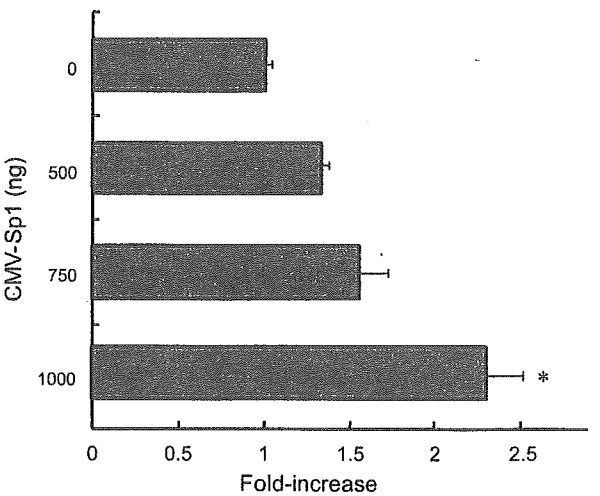

Fig. 6. Effect of Sp1 overexpression on hPEPT1 transcriptional activity. Caco-2 cells were transiently transfected with 250 ng of the −401/+60 construct and 500, 750, and 1,000 ng of the CMV-Sp1 expression vector. The total amount of transfected DNA was kept constant by adding empty vector. Data are reported as the relative fold increase compared with no CMV-Sp1 and represent the means ± SE of 3 replicates. *Significantly different from control (no CMV-Sp1; $P < 0.05$).

transcription factor through these GC-rich sites in the case of the hPEPT1 promoter.

Mutational analysis of these putative Sp1 sites revealed that mutation of Sp-A, Sp-B, or Sp-C site reduced the promoter activity. The EMSA experiment demonstrates that Sp1 binds to Sp-A and Sp-C but not to Sp-B. Collectively, these results suggest that Sp1 binds to both Sp-A and Sp-C sites and significantly contributes to the promoter activity. Although we failed to obtain evidence of the formation of a complex at the Sp-B site in EMSA, some transcription factors may interact with Sp-B and play a role in the basal promoter activity of hPEPT1. The contribution of Sp1 to the promoter activity was confirmed by a different approach, inhibition of Sp1-binding by mithramycin A and the transactivation of the promoter by overexpressed Sp1. Mithramycin A clearly reduced the promoter activity in a dose-dependent manner. Overexpression of Sp1 increased the promoter activity 2.5-fold. These results strongly indicate that Sp1 plays an essential role in the basal transcriptional regulation of hPEPT1. This regulatory mechanism for hPEPT1 was found to be similar to that of other intestinal nutrient transporters, such as Na^+-glucose transporter (SGLT1) (13) and thiamin transporter (16). In both these studies, Sp1 was shown to play a critical role through the GC-box using Caco-2 cells.

Although the present results implicated Sp1 in the basal transcriptional activity of the hPEPT1 promoter, Sp1 is not the only protein acting through GC-rich sites. Other Sp family transcription factors, such as Sp2, Sp3 and Sp4, also interact with GC-rich sites. Among them, Sp3 is ubiquitously expressed in mammalian cells (12) and has a similar affinity for the Sp1-binding site. The present results do not exclude the possibility that Sp3 might also be responsible for the transcriptional regulation of hPEPT1. In addition to Sp family proteins, Krüppel-like factor family proteins (KLFs) also bind with different affinities to GC or GT box (4). Among the Sp family, Sp1, Sp3, and Sp4 have a higher affinity for the GC box than GT box, whereas many of the KLFs bind preferentially to the GT box (4). The Sp-B site has a GT box; thus some KLFs such as GKLF, which is highly expressed in terminally differentiated epithelial cells of the intestine (23), might interact with Sp-B.

hPEPT1 protein is expressed mainly in the small intestine and, to a lesser extent, in the kidney. Although the present study revealed the contribution of Sp1 to the transcriptional regulation of hPEPT1, the mechanism of this tissue-specific expression has not been clarified yet. Computational analysis showed the presence of a binding site for a caudal related homeobox factor, Cdx, within 500 bases upstream of the transcription start site. Cdx-2 is involved in the early differentiation, proliferation, and maintenance of intestinal epithelial cells (25, 27) and in the transcription of intestinal genes, such as the sucrase-isomaltase (26), lactase-phlorizin hydrolase (15), and claudin-2 (22) genes. Although more studies are needed, Cdx-2 may be responsible for the tissue specificity of hPEPT1 expression.

In conclusion, the present results indicate that Sp1 functions as a basal transcriptional regulator of the hPEPT1 gene, and this is the first demonstration to identify the *cis* elements and *trans* factors for the regulation of a human peptide transporter. These findings should serve as a basis for future investigation into the molecular regulation of the transport of nutrient peptides and some pharmaceuticals in the human intestine and other tissues.

ACKNOWLEDGMENTS

We are grateful to Dr. R. Tjian (University of California, Berkeley) for the generous gift of Sp1 expression vector.

GRANTS

This work was supported by the 21st Century COE Program "Knowledge Information Infrastructure for Genome Science," a grant-in-aid for research on advanced medical technology from the Ministry of Health, Labor, and Welfare of Japan, and a grant from the Yamanouchi Foundation for Research on Metabolic Disorders.

REFERENCES

1. **Adibi SA.** Regulation of expression of the intestinal oligopeptide transporter (Pept-1) in health and disease. *Am J Physiol Gastrointest Liver Physiol* 285: G779–G788, 2003.
2. **Ashida K, Katsura T, Motohashi H, Saito H, and Inui K.** Thyroid hormone regulates the activity and expression of the peptide transporter PEPT1 in Caco-2 cells. *Am J Physiol Gastrointest Liver Physiol* 282: G617–G623, 2002.
3. **Berlioz F, Maoret JJ, Paris H, Laburthe M, Farinotti R, and Rozé C.** α_2-Adrenergic receptors stimulate oligopeptide transport in a human intestinal cell line. *J Pharmacol Exp Ther* 294: 466–472, 2000.
4. **Black AR, Black JD, and Azizkhan-Clifford J.** Sp1 and krüppel-like factor family of transcription factors in cell growth regulation and cancer. *J Cell Physiol* 188: 143–160, 2001.
5. **Blake MC, Jambou RC, Swick AG, Kahn JW, and Azizkhan JC.** Transcriptional initiation is controlled by upstream GC-box interactions in a TATAA-less promoter. *Mol Cell Biol* 10: 6632–6641, 1990.
6. **Blume SW, Snyder RC, Ray R, Thomas S, Koller CA, and Miller DM.** Mithramycin inhibits SP1 binding and selectively inhibits transcriptional activity of the dihydrofolate reductase gene in vitro and in vivo. *J Clin Invest* 88: 1613–1621, 1991.
7. **Buyse M, Charrier L, Sitaraman S, Gewirtz A, and Merlin D.** Interferon-γ increases hPepT1-mediated uptake of di-tripeptides including the bacterial tripeptide fMLP in polarized intestinal epithelia. *Am J Pathol* 163: 1969–1977, 2003.
8. **Daniel H.** Molecular and integrative physiology of intestinal peptide transport. *Annu Rev Physiol* 66: 361–384, 2004.
9. **Fei YJ, Sugawara M, Liu JC, Li HW, Ganapathy V, Ganapathy ME, and Leibach FH.** cDNA structure, genomic organization, and promoter analysis of the mouse intestinal peptide transporter PEPT1. *Biochim Biophys Acta* 1492: 145–154, 2002.
10. **Fujita T, Majikawa Y, Umehisa S, Okada N, Yamamoto A, Ganapathy V, and Leibach FH.** σ-Receptor ligand-induced up-regulation of the H^+/peptide transporter PEPT1 in the human intestinal cell line Caco-2. *Biochem Biophys Res Commun* 261: 242–246, 1999.
11. **Gangopadhyay A, Thamotharan M, and Adibi SA.** Regulation of oligopeptide transporter (Pept-1) in experimental diabetes. *Am J Physiol Gastrointest Liver Physiol* 283: G133–G138, 2002.
12. **Li L, He S, Sun JM, and Davie JR.** Gene regulation by Sp1 and Sp3. *Biochem Cell Biol* 82: 460–471, 2004.
13. **Martin MG, Wang J, Solorzano-Vargas RS, Lam JT, Turk E, and Wright EM.** Regulation of the human Na^+-glucose cotransporter gene, SGLT1, by HNF-1 and Sp1. *Am J Physiol Gastrointest Liver Physiol* 278: G591–G603, 2000.
14. **Mastrangelo IA, Courey AJ, Wall JS, Jackson SP, and Hough PVC.** DNA looping and Sp1 multimer links: a mechanism for transcriptional synergism and enhancement. *Proc Natl Acad Sci USA* 88: 5670–5674, 1991.
15. **Mitchelmore C, Troelsen JT, Spodsberg N, Sjostrom H, and Noren O.** Interaction between the homeodomain proteins Cdx2 and HNF1alpha mediates expression of the lactase-phlorizin hydrolase gene. *Biochem J* 346: 529–535, 2000.
16. **Nabokina SM and Said HM.** Characterization of the 5′-regulatory region of the human thiamin transporter SLC19A3: in vitro and in vivo studies. *Am J Physiol Gastrointest Liver Physiol* 287: G822–G829, 2004.
17. **Naruhashi K, Sai Y, Tamai I, Suzuki N, and Tsuji A.** Pept1 mRNA expression is induced by starvation and its level correlates with absorptive

transport of cefadroxil longitudinally in the rat intestine. *Pharm Res* 19: 1417–1423, 2002.

18. **Nielsen CU, Amstrup J, Steffansen B, Frokjaer S, and Brodin B.** Epidermal growth factor inhibits glycylsarcosine transport and hPepT1 expression in a human intestinal cell line. *Am J Physiol Gastrointest Liver Physiol* 281: G191–G199, 2001.
19. **Pan X, Terada T, Irie M, Saito H, and Inui K.** Diurnal rhythm of H^+-peptide cotransporter in the rat small intestine. *Am J Physiol Gastrointest Liver Physiol* 283: G57–G64, 2002.
20. **Pugh BF and Tjian R.** Transcription from a TATA-less promoter requires a multisubunit TFIID complex. *Genes Dev* 5: 1935–1945, 1991.
21. **Ray R, Snyder RC, Thomas S, Koller CA, and Miller DM.** Mithramycin blocks protein binding and function of the SV40 early promoter. *J Clin Invest* 83: 2003–2007, 1989.
22. **Sakaguchi T, Gu X, Golden HM, Suh E, Rhoads DB, and Reinecker HC.** Cloning of the human claudin-2 5′-flanking region revealed a TATA-less promoter with conserved binding sites in mouse and human for caudal-related homeodomain proteins and hepatocyte nuclear factor-1 alpha. *J Biol Chem* 277: 21361–21370, 2002.
23. **Shields JM, Christy RJ, and Yang VW.** Identification and characterization of a gene encoding a gut-enriched Krüppel-like factor expressed during growth arrest. *J Biol Chem* 271: 20009–20017, 1996.
24. **Shiraga T, Miyamoto K, Tanaka H, Yamamoto H, Taketani Y, Morita K, Tamai I, Tsuji A, and Takeda E.** Cellular and molecular mechanisms of dietary regulation on rat intestinal H^+/peptide transporter PepT1. *Gastroenterology* 116: 354–362, 1999.
25. **Silberg DG, Swain GP, Suh ER, and Traber PG.** Cdx1 and Cdx2 expression during intestinal development. *Gastroenterology* 119: 961–971, 2000.
26. **Suh E, Chen L, Taylor J, and Traber PG.** A homeodomain protein related to caudal regulates intestine-specific gene transcription. *Mol Cell Biol* 14: 7340–7351, 1994.
27. **Suh E and Traber PG.** An intestine-specific homeobox gene regulates proliferation and differentiation. *Mol Cell Biol* 16: 619–625, 1996.
28. **Terada T and Inui K.** Peptide transporters: structure, function, regulation and application for drug delivery. *Curr Drug Metabol* 5: 85–94, 2004.
29. **Urtti A, Johns SJ, and Sadee W.** Genomic structure of proton-coupled oligopeptide transporter *hPEPT1* and pH sensing regulatory splice variant. *AAPS Pharm Sci* 3: E6, 2001.

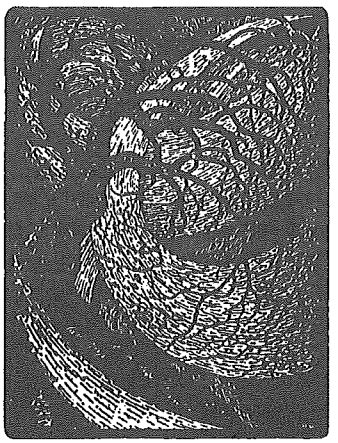

Available online at www.sciencedirect.com
SCIENCE DIRECT
Biochemical Pharmacology 70 (2005) 1104–1113
Biochemical Pharmacology
www.elsevier.com/locate/biochempharm

Human organic anion transporter hOAT3 is a potent transporter of cephalosporin antibiotics, in comparison with hOAT1

Harumasa Ueo, Hideyuki Motohashi, Toshiya Katsura, Ken-ichi Inui *

Department of Pharmacy, Kyoto University Hospital, Faculty of Medicine, Kyoto University, Kyoto 606-8507, Japan

Received 7 June 2005; accepted 29 June 2005

Abstract

We examined the substrate specificity of human organic anion transporter (hOAT) 1 and hOAT3 for various cephalosporin antibiotics, cephaloridine, cefdinir, cefotiam, ceftibuten, cefaclor, ceftizoxime, cefoselis and cefazolin by using HEK293 cells stably transfected with hOAT1 or hOAT3 cDNA (HEK-hOAT1, HEK-hOAT3). Additionally, we examined the uptake of various compounds by these transfectants. The mRNA level of hOAT3 in HEK-hOAT3 was about three-fold that of hOAT1 in HEK-hOAT1. Functional expression of hOAT1 and hOAT3 was confirmed by the uptake of *p*-[^{14}C]aminohippurate and [^{3}H]estrone sulfate, respectively. *p*-[^{14}C]Aminohippurate, [^{3}H]estrone sulfate, [^{14}C]captopril, [^{3}H]methotrexate, [^{3}H]ochratoxin A, [^{3}H]leucovorin and [^{3}H]cimetidine were shown to be substrates for hOAT1 and hOAT3, and [^{3}H]dehydroepiandrosterone sulfate was shown to be a substrate for hOAT3. All cephalosporin anitibiotics tested were shown to inhibit the uptake of *p*-[^{14}C]aminohippurate and [^{3}H]estrone sulfate via hOAT1 and hOAT3, respectively, in a dose-dependent manner, and the IC_{50} values of these antibiotics, except for cefaclor, for the hOAT1-mediated uptake of *p*-[^{14}C]aminohippurate were within four-fold of those for the hOAT3-mediated uptake of [^{3}H]estrone sulfate. The uptake of cephaloridine, cefdinir and cefotiam by HEK-hOAT3 was 35–50-fold greater than that by control cells. Moreover, the accumulation of the other cephalolsporin antibiotics was significantly greater in HEK-hOAT3 than in control cells. In contrast, the uptake of these antibiotics by HEK-hOAT1 was within two-fold of that by control cells. In conclusion, hOAT3 plays a more important role than hOAT1 in the renal secretion of cephalosporin antibiotics.

Keywords: Organic anion transporter; Cephalosporin antibiotics; *p*-Aminohippurate; Estrone sulfate; Renal secretion; Transport

1. Introduction

In the kidney, organic anion transporters, which are expressed in the apical and basolateral membranes of tubular epithelial cells, are responsible for tubular secretion of organic anions including drugs, toxins and endogenous compounds [1–3]. Cloned human organic anion transporters (hOATs) have been shown to transport clinically important drugs, such as antiviral agents [4], nonsteroidal anti-inflammatory drugs (NSAIDs) [5] and diuretics [6]. We previously reported that mRNA levels of hOAT1 and hOAT3 were much higher than those of other organic ion transporters in the human kidney cortex, and that hOAT1 and hOAT3 were localized to the basolateral membrane of the proximal tubular cells [7]. These results suggest that hOAT1 and hOAT3 play important roles in the tubular uptake of various drugs from the circulation. Therefore, for elucidation of the mechanism behind the renal elimination of various drugs, it is important to characterize the substrate specificities of these transporters.

Most cephalosporin antibiotics are excreted into urine in nonmetabolized forms, and renal tubular secretion appears to be an important pathway for their renal clearance [8]. Several in vivo and in vitro studies have tried to elucidate the transport mechanisms of cephalosporins in the kidney [9–11]. From these findings, it was suggested that OATs would be involved in the renal secretion of cephalosporins. Actually, rat OAT1 transported cephalosporins [12].

Abbreviations: hOAT, human organic anion transporter; rOAT, rat organic anion transporter

* Corresponding author. Tel.: +81 75 751 3577; fax: +81 75 751 4207.
E-mail address: inui@kuhp.kyoto-u.ac.jp (K.-i. Inui).

0006-2952/$ – see front matter © 2005 Elsevier Inc. All rights reserved.
doi:10.1016/j.bcp.2005.06.024

With regard to human OATs, Takeda et al. [13] reported that cephalosporin antibiotics interacted with hOATs. However, it has not been clarified whether hOATs are responsible for the tubular secretion of antibiotics. In our previous study, it was recognized that hOAT3 mediated the transport of cefazolin [14]. Moreover, renal excretion of cefazolin was significantly correlated with hOAT3 mRNA levels in patients with renal diseases, suggesting that hOAT3 plays an important role in the secretion of cefazolin in such patients [14]. It has remained to be elucidated whether hOAT1 or hOAT3 transports other cephalosporins.

In this study, we examined the transport of various cephalosporin antibiotics by hOAT1 and hOAT3 to characterize the substrate specificity of these transporters.

2. Materials and methods

2.1. Materials

p-[Glycyl-1-^{14}C]aminohippurate (1.9 GBq/mmol) and [1,2,6,7-^{3}H(*N*)]dehydroepiandrosterone sulfate, sodium salt (2.2 TBq/mmol) were obtained from NEN™ Life Science Products Inc. (Boston, MA). [6,7-^{3}H(*N*)]estrone sulfate, ammonium salt (2.1 TBq/mmol) was from Perkin-Elmer Life Sciences Inc. (Boston, MA). [^{14}C]captopril (115 MBq/mmol) was from Sankyo Co. (Tokyo, Japan). [3′,5′,7′-^{3}H(*N*)]methotrexate, disodium salt (851 GBq/mmol), [^{3}H(G)]ochratoxin A (666 GBq/mmol) and [3′,5′,7′,9′-^{3}H] (6*S*)-leucovorin, diammonium salt (962 GBq/mmol) were from Moravek Biochemicals Inc. (Brea, CA). [*N*-Methyl-^{3}H]Cimetidine (451 GBq/mmol) was from Amersham Biosciences (Uppsala, Sweden). Cefaclor, cephaloridine and ceftibuten (Shionogi Co., Osaka, Japan), cefdinir, ceftizoxime, cefoselis and cefazolin (Fujisawa Pharmaceutical Co., Osaka, Japan) and cefotiam (Takeda Chemical Industries, Osaka, Japan) were gifts from the respective suppliers. All other chemicals used were of the highest purity available.

2.2. Cell culture and transfection

HEK 293 cells (American Type Culture Collection CRL-1573), a transformed cell line derived from human embryonic kidney, were cultured in complete medium consisting of Medium 199 (Invitrogen, Carlsbad, CA) with 10% fetal bovine serum (Thermo. Electron Co., Waltham, MA) (Invitrogen) in an atmosphere of 5% CO_2, 95% air at 37 °C. hOAT1 and hOAT3 cDNAs were subcloned into pBK-CMV plasmid vector (Stratagene, La Jolla, CA). HEK 293 cells were transfected with hOAT1 cDNA, hOAT3 cDNA or empty vector using LipofectAMINE 2000 (Invitrogen) according to the manufacturer's instructions. G418 (Nacalai Tesque, Kyoto, Japan) (0.5 mg/ml)—resistant cells were removed. Cells expressing hOAT1 (HEK-hOAT1) were selected by measuring *p*-[^{14}C]aminohippurate uptake, and cells expressing hOAT3 (HEK-hOAT3) were selected by measuring [^{3}H]estrone sulfate uptake. Cells transfected with empty vector (HEK-pBK) were used as control cells. These transfectants were maintained in complete medium with G418 (0.5 mg/ml).

2.3. Quantification of mRNA expression of hOATs in HEK-hOAT1 and HEK-hOAT3

Total RNA was extracted from HEK-hOAT1 or HEK-hOAT3 using an RNeasy mini kit (Qiagen, Hilden, Germany) according to the manufacturer's instructions and reverse-transcribed using SuperScriptsTMII RT (Invitrogen, Grand Island, NY). For quantification of the amounts of hOAT1 and hOAT3 mRNA, the real-time PCR method was carried out using the ABI PRISM 7700 sequence detector (Applied Biosystems, Foster, CA). Glyceraldehyde-3-phosphate dehydrogenase (GAPDH) mRNA was also quantified as an internal control with GAPDH Control Reagent (Applied Biosystems).

2.4. Uptake of various compounds by HEK-hOAT1 or HEK-hOAT3

Uptake experiments were performed as described previously [15] with some modifications. HEK-hOAT1 and HEK-hOAT3 were seeded on poly-D-lysine-coated 24-well plates at a density of 2×10^5 cells/well for the uptake of *p*-[^{14}C]aminohippurate, [^{3}H]estrone sulfate, [^{14}C]captopril, [^{3}H]methotrexate, [^{3}H]ochratoxin A, [^{3}H]leucovorin, [^{3}H]cimetidine and [^{3}H]dehydroepiandrosterone sulfate. At 48 h after seeding, the uptake of these compounds by HEK-hOAT1 or HEK-hOAT3 was examined. The composition of the incubation medium was as follows (in mM): 145 NaCl, 3 KCl, 1 $CaCl_2$, 0.5 $MgCl_2$, 5 D-glucose and 5 HEPES (pH 7.4). The cells were preincubated with 0.2 ml of the incubation medium for 10 min at 37 °C. After the preincubation, the medium was replaced with 0.2 ml of incubation medium containing each anionic compound. At the end of the incubation period, the medium was aspirated, and then cells were washed two times with 1 ml of ice-cold incubation medium. The cells were lysed in 0.25 ml of 0.5N NaOH solution, and the radioactivity in aliquots was determined in 3 ml of ACSII (Amersham International, Buckingham shire, UK). The protein contents of the solubilized cells were determined by the method of Bradford [16] using the Bio-Rad Protein Assay kit (Bio-Rad, Hercules, CA) with bovine γ-globulin as a standard.

2.5. Uptake of cephalosporin antibiotics by HEK 293 cells stably expressing hOAT1 or hOAT3

For the experiments on the uptake of cephalosporin antibiotics, HEK-hOAT1 and HEK-hOAT3 were seeded

on 6-cm poly-D-lysine-coated dishes at a density of 2×10^6 cells/dish. At 48 h after seeding, the uptake of cephalosporin antibiotics was examined. The cells were preincubated with 2 ml of the incubation medium for 10 min at 37 °C. After this preincubation, the medium was replaced with 2 ml of incubation medium containing various cephalosporin antibiotics. At the end of the incubation period, the medium was aspirated, and then cells were washed three times with 5 ml of ice-cold incubation medium. To measure the accumulation of cephalosporin antibiotics, the cells were scraped and homogenized with 1 ml of water. Protein levels were determined with 5 μl of the homogenate. For the determination of cephalosporin antibiotics, to 0.9 ml of the homogenate, 100 μl of water and 20 μl of phosphoric acid were added and mixed for 30 s, then 1.0 ml of the sample was loaded onto an Oasis HLB cartridge (Waters Corporation, Milford, MA) preconditioned with 1 ml each of methanol and water. The column was washed with 1 ml of 5% methanol and cephalosporin antibiotic was eluted from the column with 1 ml of methanol. The eluate was evaporated to dry at 45–50 °C and resuspended in 200 μl of mobile phase buffer. The solution was filtered through a 0.45-μm polyvinylidene fluoride filter. The concentration of cephalosporin antibiotic was measured by use of a high performance liquid chromatograph (LC-10AT, LC-10AD, Shimadzu Co., Kyoto, Japan) equipped with a UV spectrophotometric detector (SPD-10AV, SPD-10A, Shimadzu) under the following conditions: column, Zorbax ODS column 4.6 mm inside diameter × 250 mm (Du Pont, Wilmington, DE); mobile phase, 30 mM citric acid buffer in methanol at 85:15 for cefdinir, ceftibuten, cefaclor, ceftizoxime and cefoselis, 30 mM phosphate buffer (pH 5.2) in methanol at 83:17 for cephaloridine and cefazolin, 30 mM phosphate buffer (pH 6.5) in methanol at 78:22 for cefotiam; flow rate, 0.8 ml/min; wave length, 254 nm for cephaloridine, cefotiam, ceftibuten, ceftizoxime and cefoselis, 288 nm for cefdinir, 266 nm for cefaclor, 272 nm for cefazolin; injection volume, 50 μl; temperature, 40 °C.

2.6. Statistical analysis

Data were analysed statistically using nonpaired *t*-tests.

3. Results

3.1. Construction of HEK-hOAT1 and HEK-hOAT3

In a previous study, we performed the characterization of the uptake of *p*-[^{14}C]aminohippurate and [^{3}H]estrone sulfate in HEK 293 cells transfected with hOAT1 and hOAT3 cDNA, respectively, using transient expression systems [14]. In this study, we constructed HEK 293 cells stably expressing hOAT1 or hOAT3. First, mRNA levels of hOAT1 and hOAT3 were investigated by real-time PCR. The mRNA level of hOAT1 in HEK-hOAT1 was quantified to be 64.9 amol/μg total RNA, and that of hOAT3 in HEK-hOAT3 was 225.6 amol/μg total RNA. The functional expression of hOAT1 and hOAT3 was assessed by the uptake of *p*-[^{14}C]aminohippurate and [^{3}H]estrone sulfate by HEK-hOAT1 and HEK-hOAT3, respectively. Fig. 1 shows that HEK-hOAT1 and HEK-hOAT3 exhibited time-dependent uptake of *p*-[^{14}C]aminohippurate and [^{3}H]estrone sulfate, respectively. As shown in Fig. 2, a concentration-dependent uptake of *p*-[^{14}C]aminohippurate and [^{3}H]estrone sulfate by HEK-hOAT1 and HEK-hOAT3, respectively, was observed. Using a nonlinear least squares regression analysis, kinetic parameters were calculated according to the Michaelis-Menten equation in three separate experiments. Apparent Michaelis-Menten constants (K_m) for the uptake of *p*-[^{14}C]aminohippurate by HEK-hOAT1 and of [^{3}H]estrone sulfate by HEK-hOAT3 were

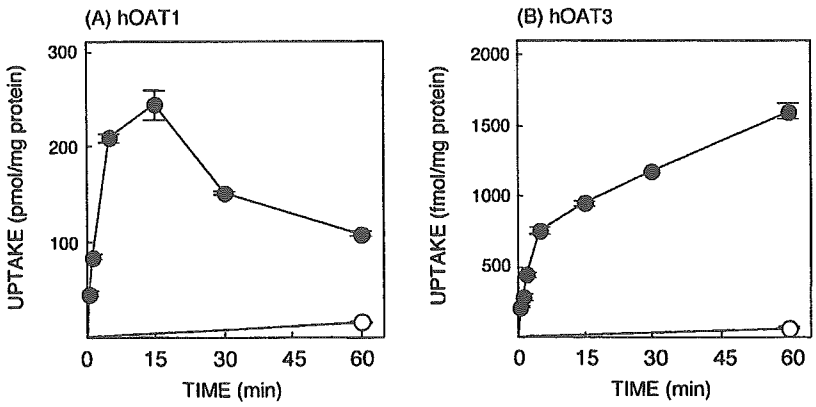

Fig. 1. Time course of *p*-[^{14}C]aminohippurate (A) and [^{3}H]estrone sulfate (B) accumulation in HEK-hOAT1 and HEK-hOAT3, respectively. (A) *p*-[^{14}C]Aminohippurate accumulation in HEK-pBK (○) or HEK-hOAT1 (●). The cells were incubated with 5 μM *p*-[^{14}C]aminohippurate for the periods indicated at 37 °C. (B) [^{3}H]Estrone sulfate accumulation in HEK-pBK (○) or HEK-hOAT3 (●). The cells were incubated with 20 nM [^{3}H]estrone sulfate for the periods indicated at 37 °C. After the incubation, the radioactivity of solubilized cells was measured. Each point represents the mean ± S.E. of three monolayers from a typical experiment.